

# CHALMERS



## Remote detection of plant stress by analysis of the dynamic behaviour of chlorophyll *a* fluorescence response

*Master's thesis in Systems, control and mechatronics*

JOHAN LINDQVIST

Department of Signals & Systems  
Systems, Control & Mechatronics  
CHALMERS UNIVERSITY OF TECHNOLOGY  
Gothenburg, Sweden 2015  
Master's Thesis EX030/2015



## Abstract

Modern greenhouses are often equipped with supplementary lighting systems, which are large consumers of electricity. In Europe alone, the power consumption of greenhouse lamps is estimated to be 100 – 200 TWh per year. Great benefits, economical and environmental, lies in making these systems more energy efficient. To this end the Swedish company Heliospectra AB is developing a complex LED-based lighting system using biological feedback to optimise the intensity and spectrum of the illumination. In this work a new method to remotely detect and track plant stress on canopy level is investigated. By tracking the stress level appropriate changes in the illumination of the plants can be made. Experiments are conducted where stress is induced in lettuce and basil plants by exposing them to different light intensities or by subjecting them to different watering schedules. An excitation light is then added to the illumination and the chlorophyll fluorescence response of the plants is analysed. The system describing these responses is found to be highly non-linear and changes with plant stress. Linear estimations of the system are made repeatedly and the dynamics of these estimations are investigated in the frequency domain. It is found that the system dynamics tend to become less complex as the plants become more stressed. Trends appear in the phase plots of the estimated systems which correlate well with stress measured by conventional plant stress measurement techniques. The method shows great promise as a candidate for remote plant stress measurements in greenhouse environments and could possibly be used in a feedback system to avoid photo inhibition.



## Preface

This work has been conducted at Heliospectra AB in a collaboration with Chalmers University of Technology, where it has been submitted for a Master of Science degree in Systems, Control and Mechatronics. The research took place during the period January 2015 - June 2015 and was supervised by Torsten Wik, Associate Professor in the Automatic control research group at Chalmers, and Daniel Båkestad, R & D Project Leader at Heliospectra.

## Acknowledgements

My gratitude goes to my advisors Torsten Wik and Daniel Båkestad. I want to thank you for giving me the opportunity to conduct this work and for the guidance and support along the way. I also want to thank PhD student Anna-Maria Carstensen, both for laying the groundwork that this thesis rest upon and for valuable discussions on the topic. To all the great employees of Heliospectra, thank you for making me feel at home at the company. Special thanks to Ida and Grazyna for advices concerning growing plants, for guiding me in the field of biology and for the nice company in the laboratory. My gratitude also to Assistant Professor Björn Lundin at Göteborgs Universitet for support concerning plant physiology and for interesting discussions about plant stress. Finally, I want to thank GU students Hampus and Emma for helping me with plant stress measurements in my experiments.

# Contents

<b>1</b>	<b>Introduction</b>	<b>1</b>
<b>2</b>	<b>Theory and litterature studies</b>	<b>4</b>
2.1	Photosynthesis and chlorophyll <i>a</i> fluorescence . . . . .	4
2.2	Chlorophyll fluorescence analysis . . . . .	5
2.3	Plant stress and stress detection . . . . .	5
2.4	Sampling . . . . .	7
2.5	Filtering and detrending . . . . .	7
2.6	Black-box modelling . . . . .	7
2.6.1	Ready-made models . . . . .	8
2.6.2	Prediction . . . . .	8
2.6.3	Fitting model parameters to measured data . . . . .	9
2.7	Frequency response and Bode plots . . . . .	10
<b>3</b>	<b>Materials</b>	<b>11</b>
3.1	Plant species . . . . .	11
3.2	Growth and experimental units . . . . .	11
3.2.1	Growth units . . . . .	11
3.2.2	Experimental units . . . . .	11
3.3	Lamps . . . . .	12
3.4	Spectrometers . . . . .	12
3.5	Fluorometers . . . . .	13
3.5.1	Junior PAM . . . . .	13
3.5.2	Pocket PEA . . . . .	14
3.6	Software . . . . .	14
<b>4</b>	<b>Methods</b>	<b>15</b>
4.1	Dynamic chlorophyll <i>a</i> fluorescence response analysis . . . . .	16
4.2	Growing plants . . . . .	17
4.2.1	Basil seeding and germination protocol . . . . .	17

4.2.2	Lettuce seeding and germination protocol . . . . .	18
4.2.3	Growth phase treatment . . . . .	18
4.2.4	Growth light regimes . . . . .	18
4.3	Stress induction . . . . .	19
4.3.1	Light stress induction . . . . .	20
4.3.2	Water stress induction . . . . .	20
4.4	Experimental measurements . . . . .	22
4.4.1	Excitation signal . . . . .	23
4.4.2	Remote sensing measurements . . . . .	25
4.4.3	Reference measurements . . . . .	25
4.4.4	Temperature measurements and fan control . . . . .	27
4.5	Data treatment . . . . .	27
4.6	System identification . . . . .	29
<b>5</b>	<b>Results and discussion</b>	<b>31</b>
5.1	Incoming light, fluorescence response and temperature measurements . . .	31
5.2	System identification . . . . .	37
5.3	Properties of the estimated systems . . . . .	41
5.4	Reference measurements . . . . .	48
5.4.1	Light stress experiments . . . . .	48
5.4.2	Water stress experiments . . . . .	50
5.5	Remote sensing versus reference measurements . . . . .	52
<b>6</b>	<b>Conclusion</b>	<b>55</b>
<b>Bibliography</b>		<b>57</b>

# 1

## Introduction

THE SWEDISH COMPANY HELIOSPECTRA AB is developing a LED-based lighting system for research purposes and for the greenhouse market. The lamps are equipped with multiple LEDs of different colours and with processor and communication capacities, enabling features for varying the intensity and spectral composition of the light. Compared to high pressure sodium (HPS) lamps traditionally used in greenhouses, which have a fixed spectrum and on/off control only, these lamps could be utilized for a more energy efficient illumination. Not only is the electrical efficiency of the LED lamps generally higher than that of the HPS lamps, but the LED lighting system could also be extended with suitable sensors enabling feedback control to optimise the energy consumption. The company is developing such a system in a collaboration with the Automatic Control Group, department of Signals and Systems, at Chalmers. The large power consumption of lighting systems used in modern greenhouses, estimated to be in the range of 100 – 200 TWh per year in Europe alone [1], highlights the importance of this research. The control system can be divided into several parts:

- Spectrum optimization - adjustment of the emitted light of the lamps to match the absorption spectrum of the plants.
- Stress detection - by measuring the stress level of the plants the lamps can be controlled to avoid excess light and photo inhibition.
- Light addition - by measuring the incoming sunlight the light intensity of the light can be automatically decreased when the background light is strong.
- Growth control - the growth rate of the plants can be manipulated by adjusting the light, with the aim to match the markets current supply and demand of the crops.

This thesis is a part of the research to develop such a control system, with focus on developing a method to remotely detect the stress level of the plants by measuring and

analysing the chlorophyll fluorescence of the plants.

Chlorophyll fluorescence analysis as a tool for measuring plant physiology is not a new field of research. The chlorophyll fluorescence is a probe into various aspects of photosynthesis [2] and analysis of it gives valuable informations about plant physiology. Fluorometers measuring parameters related to plant stress and photosynthetic efficiency have been available for some time. Most of the conventional instruments, such as the Handy PEA from Hansatech Instruments, or the Junior PAM from Walz, require hands on operation at leaf level [3, 4]. They also require dark adaptation of the plant sample to be able to determine their full range of stress related parameters. Such requirements make these instruments unsuitable for stress measurements that are to be used as feedback for lamp control in a greenhouse environment. Methods for measuring at a distance exist. The most robust of those methods is called  $\tau$ -LIDAR. However, it is expensive [5] and therefore not a suitable option for control of individual lamps in a feedback system. Another new method is the laser induced fluorescence transient (LIFT) technique, that can measure fluorescence parameters at a distance of up to 50 meters [6]. The method uses laser diodes to excite chlorophyll fluorescence in a way that is not replicable with the Heliospectra LED lamps. This motivates research of a new method to measure plant stress and photosynthetic efficiency remotely and at canopy level in ambient light.

In previous work at the company [7], research to develop such a method has been conducted. The dynamics of chlorophyll fluorescence response to a small variation in the incoming light was measured and analysed under different levels of light induced stress. The fluorescence response was measured using a spectrometer collecting the emitted light from several basil plants at canopy level. A number of different analysis methods were investigated and one of the more promising was based on the observation that the dynamics of the slow transient of the fluorescence response changed as the plants became more stressed. Estimations of the systems in terms of black-box models were made in different operating points (stress levels), and trends correlating to stress parameters were observed in the models investigated in the frequency domain.

The main purpose of this thesis is to further investigate and refine this remote stress detection technique. The hypothesis is that the dynamics of the chlorophyll fluorescence response will change with the plant stress level (partly confirmed in [7]). Experiments are conducted where the method is deployed to measure light induced and water induced stress in lettuce and basil and comparing those measurements with stress related parameters measured with conventional fluorometers. System identification and modelling of the chlorophyll fluorescence response is central to this research. A suitable way to vary the light is chosen, a data treatment procedure is determined and different black-box model types and orders are investigated for different levels of stress.

Studies have then been made where the slow dynamics of fluorescence induction curves were investigated, indicating that state transitions in the photosynthetic apparatus are an important factor affecting the appearance of the slow fluorescence dynamics [8]. State transitions are a process for balancing energy between photosystem I (PSI) and photosystem II (PSII) in photosynthetic organisms, known to relate to light harvesting efficiency [9]. However interesting, no deeper analysis of the processes active in

the plants as stress is induced are made in this work, as it is considered to be outside the scope of the thesis.

The goal of the research is to take significant steps towards being able to realise a robustly controlled lighting system for research and greenhouse purposes. In such a system, stress level measurements would be used as feedback to prevent excessive light exposure of the plants, with the promise of better crop yields as well as a more energy efficient illumination.

# 2

## Theory and litterature studies

UNDERLYING THEORY relevant for this thesis is presented in this chapter. This theoretical framework aims to give important insights of the phenomena investigated in the experiments conducted in this work. To this end, a short introduction to photosynthesis is given, as well as an introduction to plant stress and stress detection methods. Furthermore, important theory related to signal processing, such as the effects of sampling and filtering, are presented as well as the concept of *black-box modelling*.

### 2.1 Photosynthesis and chlorophyll *a* fluorescence

Photosynthesis is a process in plants and other organisms where light energy, from the sun or an artificial lighting system, is converted into chemical energy stored in the plant. A rough description of the process is important for understanding the origin and properties of the chlorophyll fluorescence signal targeted in this work.

When light is intercepted by a leaf it can be reflected, transmitted or absorbed. The absorption of light initiates the photosynthesis process where it is used to synthesise carbohydrates from CO<sub>2</sub> and water. Light energy is absorbed by antenna pigments by excitation from the molecules ground state. Chlorophyll *a* is one of the central antenna pigments and is primarily found in a structure known as photosystem II (PSII). It absorbs light mainly in the blue and red spectral region, which explains the green colour of most plants. The excitation energy is delivered to *reaction centres* where it is transformed to a chemical form. The general term for chemical reaction caused by light absorption is *photochemistry*. However, photochemistry is not the fate of all of the absorbed energy. Part of the energy will be dissipated as heat, a process known as *non-photochemical quenching* (NPQ). Another part of it will be re-emitted as light in the red and far red spectral region. This radiation is known as chlorophyll fluorescence (CF) and has one peak at wavelength 685 nm and one at 740 nm. The emission of chlorophyll

*a* fluorescence is relatively small ( $2 - 10\%$  of the absorbed light [10]), but its intricate connection with the other processes in the photosynthetic apparatus makes it suitable as a probe of physiology in photosynthetic organisms [11]. Generally the fluorescence yield is high when PQ and NPQ is low. Monitoring the chlorophyll *a* fluorescence gives insight into the photochemical efficiency and heat dissipation in a sample.

## 2.2 Chlorophyll fluorescence analysis

Analysis of the chlorophyll fluorescence is one of the most common techniques to study plant physiology. It is based on a discovery by Professor Hans Wilhelm Kautsky (born in Wien 13th April 1891, died on 15th May 1966) first presented in 1931, where an increasing intensity of fluorescence was observed for dark adapted photosynthetic cells as they were illuminated. The phenomenon is known as the Kautsky effect or fluorescence induction. At first there is a rapid (within one second) increase of fluorescence, followed by a much slower (over several minutes) decrease. The behaviour is related to the three main de-excitation pathways of absorbed light energy. During the dark adaptation all reaction centres open up and non-photochemical quenching is assumed to be absent. As the sample is illuminated energy is used for photochemistry and the reaction centres close, which results in an increasing fluorescence yield. This roughly explains the behaviour of the fast part of the fluorescence transient. The slower part of the transient is more complex to analyse as photochemical quenching, chlorophyll fluorescence and non-photochemical quenching are active in parallel.

Investigation of the fast fluorescence transient is the main focus in most conventional chlorophyll fluorescence analysis methods. The characteristics of the chlorophyll induction curve is used to calculate parameters which reflects the plant physiology. Important properties include minimum and maximum fluorescence yield measured for dark adapted and illuminated samples, where the maximum value is measured using a saturating light pulse. The value of the fluorescence yield prior to the saturating pulse is also an important property. Some of the parameters used to describe plant physiology that can be determined by measurements of the fast fluorescence transient are described in Table 2.1.

Analysis of the slow part of the fluorescence transient has been the focus of recent studies [12]. Several interconnected dynamic processes are taking place within this time-scale, making this part of the transient difficult to interpret.

## 2.3 Plant stress and stress detection

Plants that are subjected to an environment that modulates homeostasis could be considered stressed. The stress factors can be biotic or abiotic, where biotic stress is caused by living organisms such as pests, viruses or fungi. Abiotic stress arises from exposure to detrimental climate such as draught, heat or excessive light levels. Stressful environments are known to have a negative effect on the photosynthesis process in most plants (discussed in [15]) and are consequently affecting their growth, survivability and quality.

**Table 2.1:** Some of the plant physiology parameters that can be determined by measurements of the fast fluorescence transient. For a more detailed explanations of the parameters see [3] and [13]

Parameter	Calculation	Interpretation
$F_V/F_M$	Relation between the maximum and minimum fluorescence yield for dark adapted samples.	Maximum quantum yield. Maximal photochemical efficiency of PSII. Indicator of overall photosynthetic capacity [14].
$y(II)$	Relation between the maximum and minimum fluorescence yield for samples without dark adaptation.	Effective quantum yield. Fraction of energy photochemically converted in PSII [4].
$PI$	Function of parameters related to maximum quantum yield, probabilities in the electron transport chain and the number of absorbing chlorophylls per fully active reaction center.	Performance index, indicator of sample vitality. An expression indicating a kind of internal force of the sample to resist constraints from outside. [13]
$NPQ$	Relation between maximum fluorescence yield for samples with dark adaptation and maximum fluorescence yield for samples without dark adaptation.	Quantification of non-photochemical quenching. [4]
$Area$	Area above induction curve during the fast fluorescence transient.	Energy required to close all reaction centres [13].
$Tfm$	Time until maximum fluorescence is reached.	Time until maximum fluorescence is reached.

These negative effects leave traces in the chlorophyll *a* fluorescence and can therefore be measured.

The maximum quantum yield  $F_V/F_M$  is an indicator of the overall photosynthetic capacity of a sample and is often used to measure plant stress. For most plants a healthy leaf has an  $F_V/F_M$  ratio close to 0.8. A lower value indicates that a proportion of PSII reaction centres is inactivated or damaged. This phenomenon is called photoinhibition and is commonly observed in stressed plants [14]. Water stress is an exception to this as it has shown to not affect the maximum quantum yield to any major extent, as long as the water stress is relatively mild. In [11] it is proclaimed that the PSII in higher plants is highly resistant to mild water stress, explaining the invariance of  $F_V/F_M$ .

The effective quantum yield  $y(II)$  is not accepted as a measure of stress to the same extent as  $F_V/F_M$ , though a correlation between the two has been shown. Whether or

not the parameter is suitable for stress measurements, it is still an interesting parameter from an energy efficiency perspective as it represents the fraction of energy that is photochemically converted in the PSII. Low values of  $y(II)$  indicates that energy is "wasted" on other processes in the system, such as  $NPQ$ .

The Performance Index (PI) is a more complex parameter taking all of the main photochemical processes into account, making it a suitable parameter to measure photosynthetic performance of stressed plants [16].

## 2.4 Sampling

In the field of signal processing, sampling is the reduction of a continuous time signal  $y(t)$  into a discrete signal  $y[k] = y(kT)$  where  $k \in \mathbb{N}^+$ ,  $T$  is the sampling period and  $\omega_s = \frac{2\pi}{T}$  is the sampling frequency in rad/s.

The *Nyquist frequency* is described as  $\omega_N = \omega_s/2$ , and the Nyquist-Shannons sampling theorem states that if the Nyquist frequency is equal or greater than the bandwidth of the sampled signal, all information in the signal will be captured [17]. If, however, the signal contains frequencies higher than the Nyquist frequency a phenomenon called *aliasing* will occur. The alias effect springs from the fact that the spectrum of the sampled signal is periodic with period  $2\omega_N$ , with the result that frequencies in the time continuous signal higher than the Nyquist frequency will be "folded into" the lower frequency band and therefore misinterpreted as lower frequencies in the sampled signal.

## 2.5 Filtering and detrending

Filtering is the process of removing unwanted content of a signal. High frequency content can be removed using a low-pass filter. Such a filter passes signal content with frequency below the *cut-off frequency* and attenuates higher frequency content. The cut-off frequency is defined as the breakpoint at which frequencies are attenuated by  $-3$  dB of the nominal passband value. The cut-off frequency and the attenuation at different frequencies depends on the filter design.

A trend in a time series is a slow change of the local mean over the whole time interval under investigation. Essentially, trends are low frequency signal content and *detrending* is the process of removing such content. This can be achieved by subtracting a suitable interpolation of the slow change from the data, often in the form of a least square fit of a line or a spline.

## 2.6 Black-box modelling

Black-box modelling is a modelling procedure that requires no physical insight into the system. Standard models that are known to handle a wide range of system dynamics are fitted to measured data.

### 2.6.1 Ready-made models

The models that are fitted to the collected data in the black-box modelling are called *ready-made models* and come in different forms. The most general linear model structure normally used is known as the Box-Jenkins model and is described by

$$y(t) = \frac{B(q^{-1})}{F(q^{-1})}u(t) + \frac{C(q^{-1})}{D(q^{-1})}e(t), \quad (2.1)$$

where  $y(t)$  is the system's measured output,  $u(t)$  is the input and  $e(t)$  is a disturbance.  $B$ ,  $F$ ,  $C$  and  $D$  are polynomials in the time shift operator  $q^{-1}$ . The fraction  $B(q^{-1})/F(q^{-1})$  defines the process model, often denoted  $G(q^{-1})$ , and the fraction  $C(q^{-1})/D(q^{-1})$  defines the disturbance model ( $H(q^{-1})$ ). The orders of the polynomials are determined by the parameters  $nb$ ,  $nf$ ,  $nc$  and  $nd$ , and a time delay of  $nk$  samples can be specified. The order of the polynomials  $B(q^{-1})$  and  $F(q^{-1})$  defines the number of zeros and poles for the process model, while the order of the polynomials  $C(q^{-1})$  and  $D(q^{-1})$  defines the number of zeros and poles for the disturbance model. A time delay will appear in the model as a shift towards a higher order of the polynomial  $B(q^{-1})$ . Different model complexities can be obtained by certain choices of polynomials. The least complex model, the ARX (Auto Regressive with eXogeneous input) model, is obtained when  $D(q^{-1}) = F(q^{-1})$  and  $C(q^{-1}) \equiv 1$ , giving

$$F(q^{-1})y(t) = B(q^{-1})u(t) + e(t). \quad (2.2)$$

The ARX model parameters are easy to estimate since the corresponding estimation problem is of linear regression type. However, it has the rigidity of sharing poles between the process model and the disturbance model. Additional flexibility to describe the disturbance model can be obtained by a higher order of the polynomial  $C(q^{-1})$ , giving an ARMAX (Auto Resgressive Moving Average with eXogenous input) model

$$A(q^{-1})y(t) = B(q^{-1})u(t) + C(q^{-1})e(t). \quad (2.3)$$

If the properties of the disturbance signals are not model, i.e.  $C(q^{-1})/D(q^{-1}) \equiv 1$ , an OE (Output Error) model is obtained

$$y(t) = \frac{B(q^{-1})}{F(q^{-1})}u(t) + e(t). \quad (2.4)$$

In an OE model no parameters are wasted on modelling the disturbance. If the system operates without feedback during the data collection, a correct description of the process model  $G(q^{-1})$  can be obtained regardless of the noise [18].

### 2.6.2 Prediction

With the models described by (2.1) – (2.4) it is possible to predict the output  $y(t)$  based on prior measurements of the system input and output. The disturbance signal

$e(t)$  represents a white noise and cannot be predicted. The prediction of the output is denoted as

$$\hat{y}(t|\boldsymbol{\theta}), \quad (2.5)$$

where  $\boldsymbol{\theta} = [a_1 \ a_2 \ \dots \ a_{na} \ b_1 \ b_2 \ \dots \ b_{nb} \ c_1 \ c_2 \ \dots \ c_{nc} \ d_1 \ d_2 \ \dots \ d_{nd}]^T$  is the *parameter vector* containing the coefficients of the model polynomials. The complexity of the prediction (2.5) depends on which model is used. In the case of an ARX model, the prediction is a linear function of  $\boldsymbol{\theta} = [a_1 \ a_2 \ \dots \ a_{na} \ b_1 \ b_2 \ \dots \ b_{nb}]$

$$\hat{y}(t|\boldsymbol{\theta}) = \boldsymbol{\theta}^T \boldsymbol{\phi}(t),$$

where  $\boldsymbol{\phi}(t) = [-y(t-1) \ \dots \ -y(t-na) \ u(t-nk) \ \dots \ u(t-nk-nb+1)]^T$  is the *regression vector* containing prior measurements of the system input and output.

In the OE model case the prediction is simply the model without the noise  $e(t)$ , giving

$$\hat{y}(t|\boldsymbol{\theta}) = \frac{A(q^{-1})}{B(q^{-1})} u(t),$$

which is based solely on the inputs of the systems and not on old values of the output.

### 2.6.3 Fitting model parameters to measured data

The prediction (2.5) depends on  $\boldsymbol{\theta}$  and for every choice of parameter vector a prediction  $\hat{y}(t|\boldsymbol{\theta})$  of the signal  $y(t)$  can be made at time  $t - 1$ . To find the optimal choice of  $\boldsymbol{\theta}$  an optimization problem has to be solved. To this end the *prediction error* is calculated as

$$\epsilon(t|\boldsymbol{\theta}) = y(t) - \hat{y}(t|\boldsymbol{\theta}).$$

With input and output data collected over a period  $t = 1, 2, \dots, N$  a cost function is formed as

$$V_N(\boldsymbol{\theta}) = \frac{1}{N} \sum_{t=1}^N \epsilon^2(t|\boldsymbol{\theta}), \quad (2.6)$$

measuring how well the parameter  $\boldsymbol{\theta}$  performs. The optimal vector  $\boldsymbol{\theta}^*$  is the one that minimises the cost function, i.e:

$$\boldsymbol{\theta}^* = \arg \min_{\boldsymbol{\theta}} V_N(\boldsymbol{\theta}).$$

Minimisation of the cost function (2.6) can be solved analytically in the case of an ARX model. However, for most model structures the cost function is rather complicated and is solved numerically using iterative methods such as the Newton-Raphson method or similar. Estimation of an ARX model normally has a unique solution whereas the numerical solutions of more complicated models may depend on the initial guess of the parameter vector [7].

## 2.7 Frequency response and Bode plots

The dynamics of a linear system or model can be characterised by its frequency response. It presents the systems response to stimulus at different frequencies. The frequency response of a process model  $G(q^{-1})$  is obtained by replacing the argument  $q$  with  $e^{i\omega}$ , where  $\omega$  is the angular frequency. The frequency response can be visualised by calculating the magnitude  $|G(i\omega)|$  and the phase  $\angle G(i\omega)$  and plotting them against the angular frequency. Such diagrams are known as Bode plots.

# 3

## Materials

**T**HIS CHAPTER presents materials and setups used in this work, such as plants, lamps, spectrometers and fluorometers. Pots, trays and other equipment used for growing plants are excluded. All computer software used is presented in the last section of this chapter.

### 3.1 Plant species

Experiments were conducted on two plant species, namely Aroma 2 Basil (*Ocimum basilicum*) and Amerikanischer Brauner Lettuce (*Lactuca sativa*). Both species are commonly grown in greenhouse production, motivating the choice of these particular species. Also, previous work at the company [7] and [19] has been conducted on other varieties of basil. The seeding and growing protocols for the plants are presented in detail in Section 4.2.

### 3.2 Growth and experimental units

Two types of units were used for growing plants and conducting experiments.

#### 3.2.1 Growth units

The plants were grown in *growth units* made of highly reflective curtains, measuring  $125 \times 125$  cm and an approximate height of 250 cm. The plants were placed on a metal grid 32 cm above the floor and lamps were mounted about 180 cm above the grid.

#### 3.2.2 Experimental units

Experiments were conducted in two *experiment units*, one for remote sensing and one for reference measurements. These units were Styrofoam boxes with neither top nor

bottom. The inner dimensions of the boxes (WDH) were approximately  $70 \times 70 \times 90$  cm. The boxes were placed on a metal grid 32 cm above the floor and two lamps were mounted at a height of 97.5 cm above the metal grid. The purpose of the experimental units was to increase the maximum light intensity, as well as shielding the plants from ambient light.

In the remote sensing unit two spectrometers were used. One facing up to measure the incoming light from the lamps and one facing down to measure the fluorescence from the plants. This box also had a TEMPPer USB thermometer for temperature measurements.

In the reference measurement unit three junior-PAM fluorometers (Walz) and one Pocket PEA fluorometer (Hansatech Instruments) where used to monitor the plants.

### **3.3 Lamps**

In this project two different types of Heliospectra lamps were used. In the growth units L4A S-1 custom lamps were used, with exception of the growth units used in the complementary light stress experiments where LX602 lamps were used in the growth units. The LX602 lamps were also used in the experiment units.

The L4A S-1 custom lamps have four LED groups with wavelength peaks at 450 nm, 530 nm, 660 nm and 735 nm. Each LED group's intensity level can take relative values in the range 1 to 1000, and are controlled from a computer connected to the same network. These lamps have an active cooling system with four thermometers and four fans. The fans are controlled using a simple bang-bang controller with hysteresis at  $[40.0 \pm 0.5^\circ\text{C}]$ .

The LX602 lamps have three LED groups with wavelength peaks at 450 nm, 660 nm and 6500 K (white light). These lamps are controlled in a similar fashion as the L4 lamps. The cooling system of the LX602 lamps only consists of one thermometer and one fan, but uses the same type of bang-bang controller as the L4A S-1 custom lamps for regulating the temperature.

### **3.4 Spectrometers**

To measure light three different spectrometers from Ocean Optics were used. In the experiments two Maya2000 Pro were employed and for pre experimental measurements of light regimes a Jaz spectrometer was used. These spectrometers covers the spectral range of the lamps, the photosynthetically active radiation (PAR) and the far red radiation of the chlorophyll fluorescence. They all have a good dispersion, i.e. they are able to distinguish between light of different wavelengths with a satisfactory resolution. A variable integration time allows for the user to make a trade off between signal strength and sampling rate. Some of the most important specifications of the spectrometers are presented in Table 3.1.

The first Maya2000 Pro spectrometer (M1) was used to measure the incoming light from the lamps. It was equipped with an optical fiber with a diameter of  $50 \mu\text{m}$  and a cosine corrector to increase the field-of-view from  $25^\circ$  to  $180^\circ$ . The second Maya2000 Pro spectrometer (M2) was used to measure the chlorophyll fluorescence from the plants.

**Table 3.1:** Spectrometer specifications

Spectrometer	Spectral range (nm)	Dispersion (nm pixel <sup>-1</sup> )	Integration time
Maya2000 Pro (M1)	200-1119	0.45	13 $\mu$ s – 5 s
Maya2000 Pro (M2)	119-1119	0.43	7.2 $\mu$ s – 5 s
Jaz	340-1024	0.77	870 $\mu$ s – 65 s

This spectrometer was equipped with a 600  $\mu$ m optical fiber and a Gershun tube to decrease the field-of-view from 25° to 10°, focusing the sensor on to the canopy of the plants.

When using a spectrometer it is important to correct for dark-zero readings, caused by electrical and thermal noise in the spectrometer. The dark-zero spectrum could be measured by taking a spectrometer reading in absence of light. Correction for dark-zero is then a simple subtraction of the dark-zero spectrum from the in light measurements. However, the dark-zero spectrum is not static but vary with temperature, integration time and running time. It is therefore problematic to make on-line corrections for dark-zero.

## 3.5 Fluorometers

In the experiments conducted in this work two types of fluorometers were used for reference measurements of plant physiology, namely the previously mentioned Junior PAMs and the Pocket PEA. Both instruments take measurements at leaf level and require dark adaptation of the samples to determine many of the parameters they measure correctly.

### 3.5.1 Junior PAM

A Junior PAM is a handy, price-worthy instrument for measurements of plant physiology. It is to be connected to a sample via a plastic fibre with a diameter of 1.5 mm. A blue (450 nm) LED is employed for pulse modulated fluorescence excitation, actinic illumination and saturating pulses. The actinic light photon flux densities at 1 mm distance from the tip of the plastic fibre is adjustable in the range of 25 – 1500  $\mu$ mol photons/m<sup>-2</sup>s. The saturating pulse at the same distance has a maximum photon flux density of 10000  $\mu$ mol photons/m<sup>2</sup>s. A PIN-photodiode with a long-pass filter (50% transmission at 645 nm) is used to measure the fluorescence response. Characteristics of the fluorescence response is used to calculate photosynthetic parameters such as  $F_V/F_M$ ,  $qP$ ,  $qL$ ,  $qN$ ,  $NPQ$ ,  $y(II)$ ,  $y(NPQ)$ ,  $y(NO)$  and  $ETR$ .

**Table 3.2:** List of all software used in this work.

Software	Application
MATLAB 2015b	Operating lamps and sampling spectrometers during experiments. Data treatment. System identification.
Spectrasuite	Maya2000 Pro spectrometer measurements of light regimes.
Jaz tools	Jaz spectrometer measurements of light regimes.
Heliospectra System Assistant	Manual control of Heliospectra lamps.

### 3.5.2 Pocket PEA

The Pocket PEA is a hand-held easy-to-use chlorophyll fluorometer suitable for teaching, research and commercial applications. The instrument uses a high intensity focused LED that provides an excitation light with an intensity of up to  $3500 \mu\text{mol}/\text{m}^2\text{s}$  with a peak wavelength of 627 nm at the sample surface. A sensitive PIN photodiode is used as a detector, sampling data at 10  $\mu\text{s}$  intervals during the first 300  $\mu\text{s}$  and is then switched to slower acquisition rates as the kinetics of the fluorescence signal slow. This provides high resolution of the chlorophyll induction while keeping the data set small. The Pocket PEA comes with a small leaf clip that is to be attached to the measured sample. The leaf clip has a small shutter plate which could be used to dark-adapt the target leaf area prior to the measurements. The Pocket PEA provides several photosynthetic parameters such as  $F_V/F_M$ ,  $T_{fm}$ ,  $Area$ ,  $RC/ABS$  and  $PI$ .

## 3.6 Software

The softwares used in the analysis part of this work and for operating the lamps, spectrometers and fluorometers are presented in Table 3.2.

# 4

## Methods

P LANT STRESS EXPERIMENTS are central in this work. The experiments aim to investigate the dynamic behaviour of chlorophyll *a* fluorescence response of a group of plants and determine if it can be used to quantify the stress level of the plants. The method used in this analysis, described in Section 4.1, has been investigated in previous work at the company [7]. The main objective of this thesis is to verify these results and further develop the method. The general idea of the investigations conducted for that purpose can be described in a few steps:

1. First, stress is induced in a group of plants.
2. Add a small variation in the illumination of the plants.
3. Measure and analyse the dynamic behaviour of chlorophyll *a* fluorescence response.
4. Measure plant stress using conventional methods for reference.
5. Correlate the results.

Three main experiments were carried out on basil and lettuce separately. In two experiments the plants were subjected to different light intensity levels to induce stress and in one experiment different levels of watering were used to induce stress. The method of stress induction is used to label the experiments; the *light stress experiment*, the *complementary light stress experiment* and the *water stress experiment*. An important difference between the light stress experiments and the water stress experiments was that in the latter, stress was induced prior to the experimental measurements, whereas in the light stress experiments the stress induction and experimental measurements coincide. In the complementary light stress experiments no reference measurements were taken, as they were conducted to verify and further investigate the trends that were observed in the first light stress experiments. An overview of the experiments conducted in this work is shown in Table 4.1.

**Table 4.1:** Overview of the experiments conducted in this work, showing how stress is induced and what measurements are taken in each experiment. All experiments are conducted on lettuce and basil separately.

Experiment	Stress induction	Measurements
Light stress	Light intensity	Incoming light, fluorescence response and reference measurements
Complementary light stress	Light intensity	Incoming light and fluorescence response
Water stress	Draught	Incoming light, fluorescence response and reference measurements
	Moderate watering	Incoming light, fluorescence response and reference measurements
	Excessive watering	Incoming light, fluorescence response and reference measurements

This chapter is divided into several sections describing the analysis methods, the experiments and how the plants were grown.

## 4.1 Dynamic chlorophyll *a* fluorescence response analysis

In this thesis a new method to remotely measure stress is investigated and developed. The method is based on taking measurements of the chlorophyll *a* fluorescence response, which is triggered by applying an excitation signal to the plant illumination. The term "fluorescence response" refers to a fluorescence induction like behaviour, with the exception that the illumination does not change from darkness into light but between two different light intensity levels. The behaviour of the measured fluorescence response is changing with plant stress, wherefore it is referred to as dynamic.

With measurements of the chlorophyll *a* fluorescence response and the intensity of the varying incoming light, the system can be estimated by fitting ready-made models to the data as described in Section 2.6. Since the system is continuously changing, new models are estimated periodically. These models are linear approximations of the system in different operating points. Investigation of the models in the frequency domain is conducted by inspection of their Bode diagrams. The frequency range  $0.01 - 1$  rad/s is prioritised since it has been shown to contain interesting information about photosynthesis [7].

The method is referred to as Dynamic Fluorescence Response Analysis, abbreviated DFRA. Figure 4.1 shows a schematic overview of the DFRA procedure.

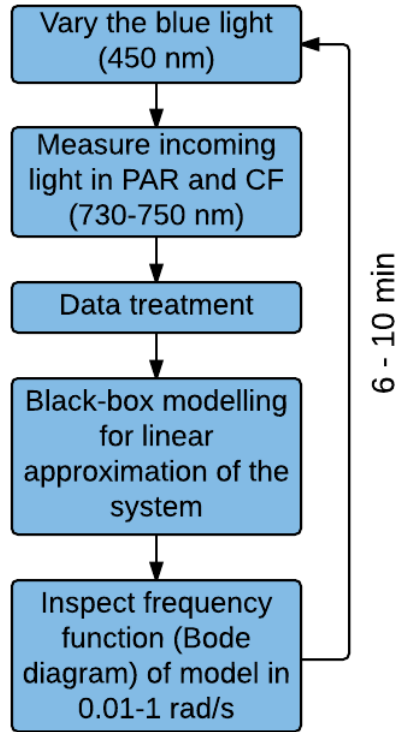


**Figure 4.1:** Schematic overview of the Dynamic Fluorescence Response Analysis procedure.

## 4.2 Growing plants

All plants used in this work were brought up from seed in a controlled environment. The protocols used for seeding and germinating basil and lettuce are presented below, as well as a description of the growth phase treatment.

#### 4.2.1 Basil seeding and germination protocol

Mix two parts soil (Proveen Substrate, Mixture Semis Bouturage 2) with one part Vermiculite (Agra) and add 1/12 L of water for each litre of soil mix. The day before seeding, add the soil mix to the pots (rectangular 0.28 L), place the pots on trays and water from below by filling the trays with water. Spray water on top of the pots to increase moisture. When seeding, spread 15 seeds evenly distributed in each pot. Spray the surface with water and cover with plastic. Place under cold fluorescent light with a photoperiod of 24 hours, with temperatures in the range of 22 – 27°C. After four days,

remove the plastic cover. Two days later, remove all seeds that has not yet germinated and remove the worst looking seedlings so that ten remain in each pot.

#### **4.2.2 Lettuce seeding and germination protocol**

Mix two parts soil (Proveen Substrate, Mixture Semis Bouturage 2) with one part Vermiculite (Agra) and add 1/12 L of water for each litre of soil mix. The day before seeding, add the soil mix to the pots (rectangular 0.28 L), place the pots on trays and water from below by filling the trays with water. Spray water on top of the pots to increase moisture. When seeding, place 4 seeds close to the middle of each pot. Spray the surface with water and cover with plastic. Place under cold fluorescent light with a photoperiod of 24 hours, with temperatures in the range of 22 – 26 °C. After four days, remove the plastic cover. On the following day, remove all seeds that has not yet germinated and remove the worst looking seedlings so that one remains in each pot.

#### **4.2.3 Growth phase treatment**

After germination the plants were randomly redistributed on the trays and moved into the growth units in the laboratory where they were subjected to their respective growth light regimes, as presented in Section 4.2.4. The photo periods in the growth units were 16 hours. The laboratory day/night temperatures were held at 22/17 °C and the air humidity was held at 60%. As the plants grew larger, they were split up on more trays. The plants were watered from below every other day by filling the trays with a mixture of water and nutrient mix (Plant-Prod All Purpose 20-20-20 Fertilizer (1 g/L), magnesium sulphate anhydrous 157 mg/L (Kali) and calcium nitrate 227 mg/L (Calcinit, YaraLiva). NPK (oxide) was 235-200-201). When getting larger, the lettuce plants were sprayed in addition to the watering to avoid tip burn of the leafs.

#### **4.2.4 Growth light regimes**

The light regimes used for growing plants were measured with an Ocean Optics Jaz spectrometer. The spectrometer was present in the middle of each growth unit, with the probe 16.5 cm above the metal grid. No plants were placed in the units when the light regimes were measured.

Three different light regimes were used during the growth phases of this project. The first (GLR lettuce) was used for growing lettuce for the light stress and the water stress experiments. The second (GLR basil) was used for growing basil for the same experiments. For these growth light regimes the L4A S-1 custom lamps were used to achieve the desired spectra and intensity levels. The third growth light regime (GLR comp) was used for growing basil and lettuce for the complementary light stress experiment. Here, Heliospectra LX602 lamps were used. The most important properties of the growth light regimes are presented in Table 4.2 and the spectra are shown in Figure 4.2.

**Table 4.2:** Properties of the light regimes used for growing plants. PAR designates the spectral range from 400 nm to 700 nm and is expressed in  $\mu\text{Ein}/\text{m}^2/\text{s}$ . Blue, green and red designates the spectral range from 400–500 nm, 500–600 nm and 600–700 nm respectively.

Light regime	PAR	Blue:Red	%Green
GLR lettuce	173	1:3.0	9.8
GLR basil	202	1:3.0	9.9
GLR comp	190	1:3.0	9.9

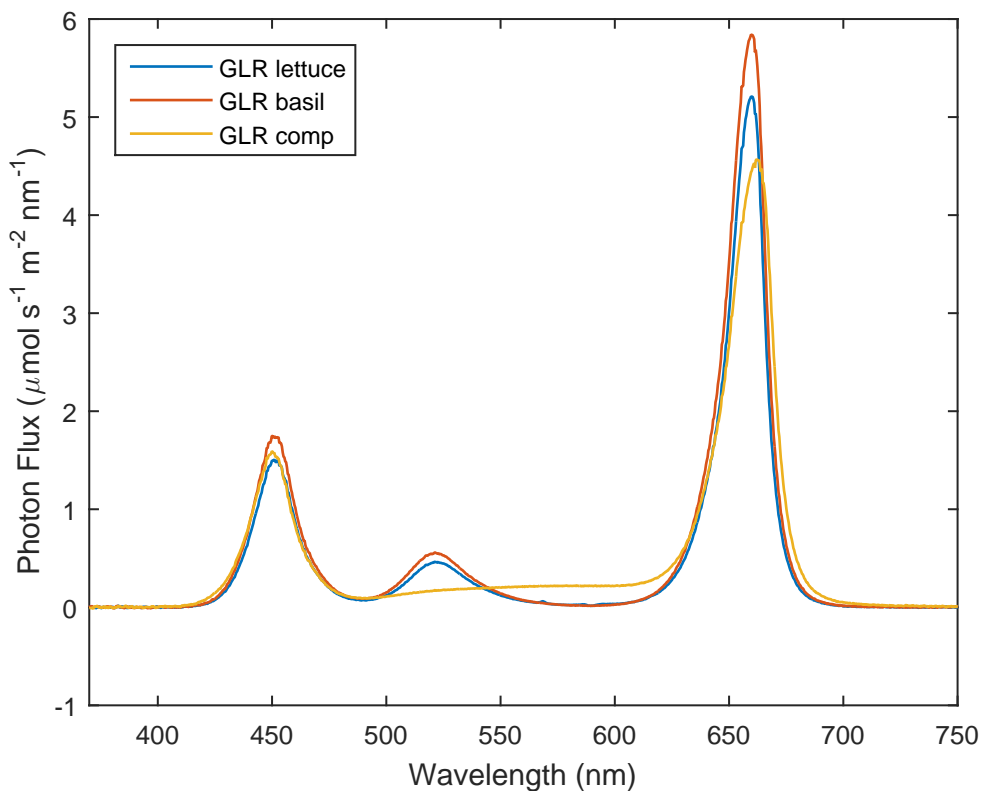


**Figure 4.2:** Growth light regimes.

### 4.3 Stress induction

The way in which stress was induced in the plants is the main difference between the experiments conducted in this work. In the light stress experiments and the complementary light stress experiments the plants were subjected to different levels of illumination to induce stress. In the water stress experiments the plants were given different amounts of water the days prior to the experimental measurements.

### 4.3.1 Light stress induction

In the light stress and the complementary light stress experiments different light intensity levels were used as background light in the experimental units. The intensity was initially low and then gradually increased to induce stress. Lastly the light intensity level was again set low, so that stress recovery of the plants could be monitored.

In the first light stress experiments eight levels ranging from approximately 100 to 1700  $\mu\text{Ein}/\text{m}^2/\text{s}$  in PAR were used. The levels were measured prior to the experimental measurement and were set to be close to equal in the remote sensing unit and the reference measurement unit. As for the growth regimes the spectrometer was placed in the middle of each unit with the probe 16.5 cm above the metal grid. No plants were placed in the units when the light regimes were measured. Table 4.3 presents the intensity levels in detail and Figure 4.3 shows the spectra as measured in the remote sensing unit. For the lettuce (l) light stress experiment levels 1-2l-3-4-5-6-7-8l were used and for the basil (b) light stress experiment levels 1-2b-3-4-5-6-7-8b were used. Each level was held for one hour. The last levels (8l and 8b) are lower intensity levels for studies of the plant stress recovery process.

In the complementary light stress experiments a different set of light intensity levels were used. The intensity of the levels ranged from approximately 200 to 900  $\mu\text{Ein}/\text{m}^2/\text{s}$  in PAR, where some were chosen to match the levels from the first light stress experiments. Only the remote sensing unit was used in these experiments, as no reference measurements were taken. The light regimes used are presented in detail in Table 4.4 and the spectra are shown in Figure 4.4. For the lettuce experiment light levels 1l-2-3-4-5-6-7-8-1l were used and for the basil experiment 1b-2-3-4-5-6-7-8-1b were used. Note that the first levels are reused again at the end of the experiment, for studies of plant stress recovery. In the complementary light stress experiments each level was held for 24 minutes.

### 4.3.2 Water stress induction

To induce water stress different watering schedules were used. Samples from each species, grown under identical conditions, were divided into three groups that were treated differently during a *stress induction phase* and measured separately in the experiments. For lettuce the stress induction period was five days and for basil it was nine days. The groups were exposed to *draught*, *moderate watering* and *excessive watering* respectively. Plants exposed to draught were given very little or no water at all during the stress induction period. The moderately watered group was kept on a "normal" watering schedule where water were given when the soil began to dry up. The excessively watered plants had their pots standing on saturated trays for the entire stress induction period. The same water-nutrient mixture used during the growth phase was used during the water stress induction, implying that the plant groups received different amounts of nutrients. This is to be kept in mind as it is a cofactor in the stress induction. The effects of the different water treatments on the appearance of the plants are shown in Figure 4.5.

**Table 4.3:** Properties of the light regimes used in the light stress and water stress experiments. PAR designates the spectral range from 400 nm to 700 nm and is expressed in  $\mu\text{Ein}/\text{m}^2/\text{s}$ . Only the second and the eighth levels differ between the lettuce (l) and basil (b) experiments. Blue, green and red designates the spectral range from 400 – 500 nm, 500 – 600 nm and 600 – 700 nm, respectively.

Unit:	Remote			Reference		
	Light regime	PAR	Blue:Red	%Green	PAR	Blue:Red
Level 1	100	1:3.0	10.7	103	1:2.9	10.7
Level 2l	175	1:3.0	10.9	175	1:2.9	11.0
Level 2b	205	1:3.1	10.8	205	1:3.0	10.1
Level 3	510	1:3.0	9.9	511	1:3.0	10.2
Level 4	717	1:3.0	10.3	716	1:3.1	10.5
Level 5	1015	1:2.9	10.3	1010	1:3.0	10.2
Level 6	1378	1:3.0	9.9	1376	1:3.1	9.9
Level 7	1699	1:3.0	10.6	1700	1:3.1	11.3
Level 8l	568	1:2.7	11.4	605	1:2.6	11.0
Level 8b	205	1:3.1	10.8	205	1:3.0	10.1

**Table 4.4:** Properties of the light regimes used in the complementary light stress experiments. PAR designates the spectral range from 400 nm to 700 nm and is expressed in  $\mu\text{Ein}/\text{m}^2/\text{s}$ . Only the first level differs between the lettuce (l) and basil (b) experiments. Blue, green and red designates the spectral range from 400 – 500 nm, 500 – 600 nm and 600 – 700 nm, respectively.

Light regime	PAR	Blue:Red	%Green
Level 1l	174	1:3.2	10.5
Level 1b	203	1:3.1	14.7
Level 2	286	1:2.8	9.1
Level 3	346	1:2.9	10.1
Level 4	423	1:3.0	9.7
Level 5	510	1:3.0	10.2
Level 6	603	1:3.0	9.9
Level 7	716	1:2.9	9.6
Level 8	880	1:3.0	9.6

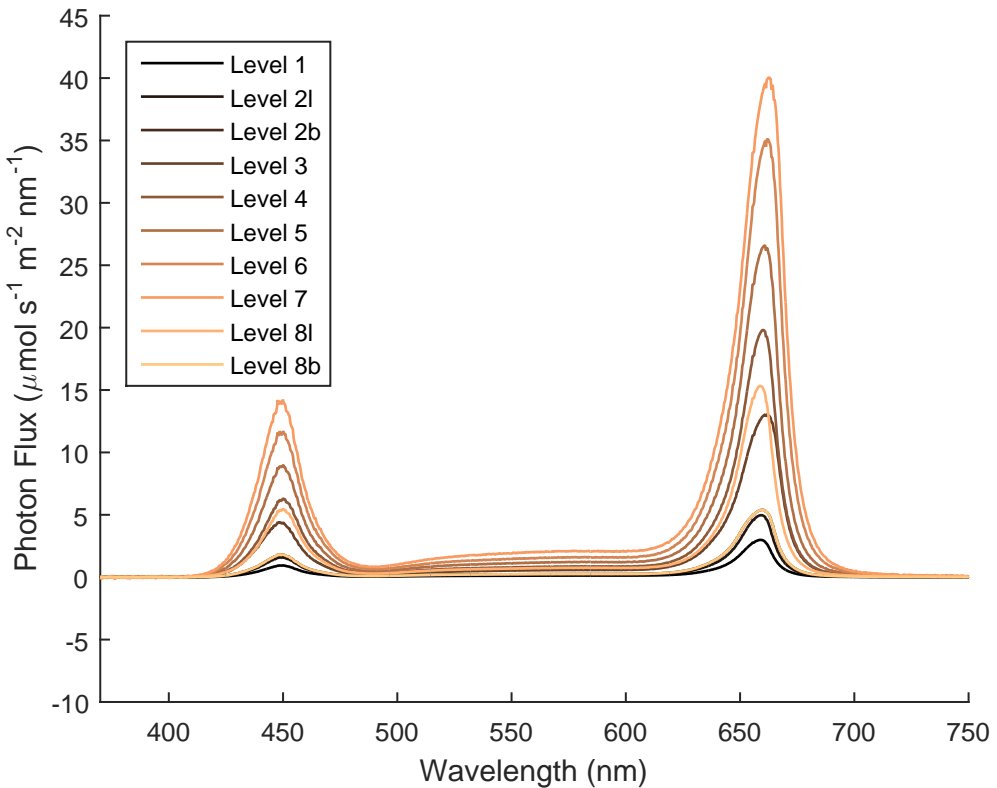


**Figure 4.3:** Spectra of the light regimes used in the light stress and water stress experiments, as measured in the remote sensing unit.

## 4.4 Experimental measurements

In the remote sensing unit the fluorescence response and the incoming light were measured, data later used in the system identification process. Reference measurements were taken in the reference measurement unit for monitoring plant physiology. Lamp temperatures and the temperature in the remote sensing unit were logged during all experimental measurements.

In each of the light stress experiments a batch of samples grown under identical conditions were randomly divided between the remote sensing unit and the reference measurement unit. Stress was induced in the plants as described in Section 4.3.1 in both units simultaneously. To trigger the fluorescence response at each level small changes in the illumination were made. This *excitation signal* is described in more detail in Section 4.4.1. Remote sensing measurements and reference measurements were taken in parallel under the assumption that the conditions in both units could be considered equal during the experiment. No reference measurements were taken in the complementary light stress experiments.

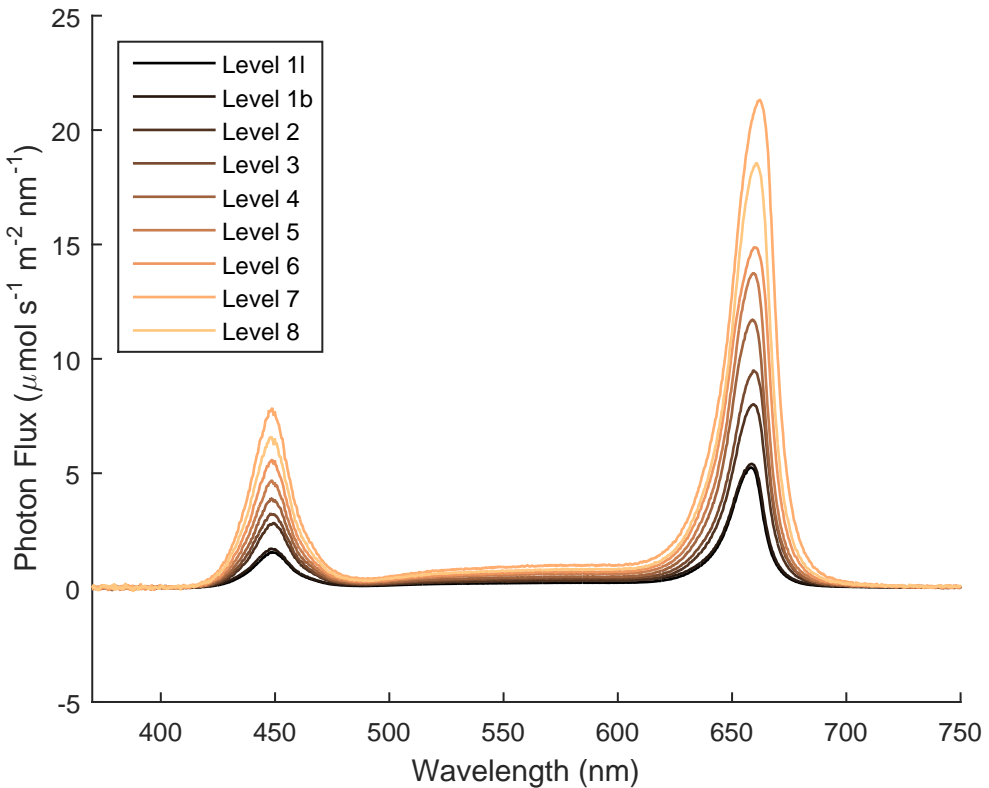


**Figure 4.4:** Spectra of the light regimes used in the complementary light stress experiments.

In the water stress experiments the reference measurements were taken prior to the remote sensing measurements, and not in parallel as in the light stress experiment. The stress induced by the different water schedules of each group is assumed to be unaffected by the reference measurements. Remote sensing measurements were taken on the plants in the remote sensing unit, where they were subjected to a light regime that matched the one they were grown under. These light regimes are presented in Table 4.5 and Figure 4.3. As for the light stress experiments an excitation signal (Section 4.4.1) was added to the respective light regime to trigger the fluorescence response. Each group of plants (draught, moderately watered and excessively watered) were measured separately.

#### 4.4.1 Excitation signal

During the experiments an excitation signal was applied to each light regime by varying the intensity of the blue (450 nm) LED group in the LX602 lamps. The excitation signal was put in the blue part of the PAR spectra to make sure that it would not overlap with the chlorophyll fluorescence peak at 740 nm that is to be measured in the remote sensing unit. The excitation signal had the form of a square wave with levels of  $\pm 30 \mu\text{Ein}/\text{m}^2/\text{s}$



**Figure 4.5:** Effects of water stress treatment for lettuce (top) and basil (bottom). The two leftmost plants were subjected to excessive watering, the two in the middle were watered normally and the two rightmost were subjected to draught. The photographs were taken after the experimental measurements.

**Table 4.5:** Properties of the light regimes used in the water stress experiments. PAR designates the spectral range from 400 nm to 700 nm and is expressed in  $\mu\text{Ein}$ . Blue, green and red designates the spectral range from 400 – 500 nm, 500 – 600 nm and 600 – 700 nm respectively.

Unit:	Remote			Reference		
	PAR	Blue:Red	%Green	PAR	Blue:Red	%Green
Lettuce	175	1:3.0	10.9	175	1:2.9	11.0
Basil	205	1:3.1	10.8	205	1:3.0	10.1

in PAR. The period of the square wave was 10 minutes in the light stress experiments and 6 minutes in the water stress and the complementary light stress experiments.

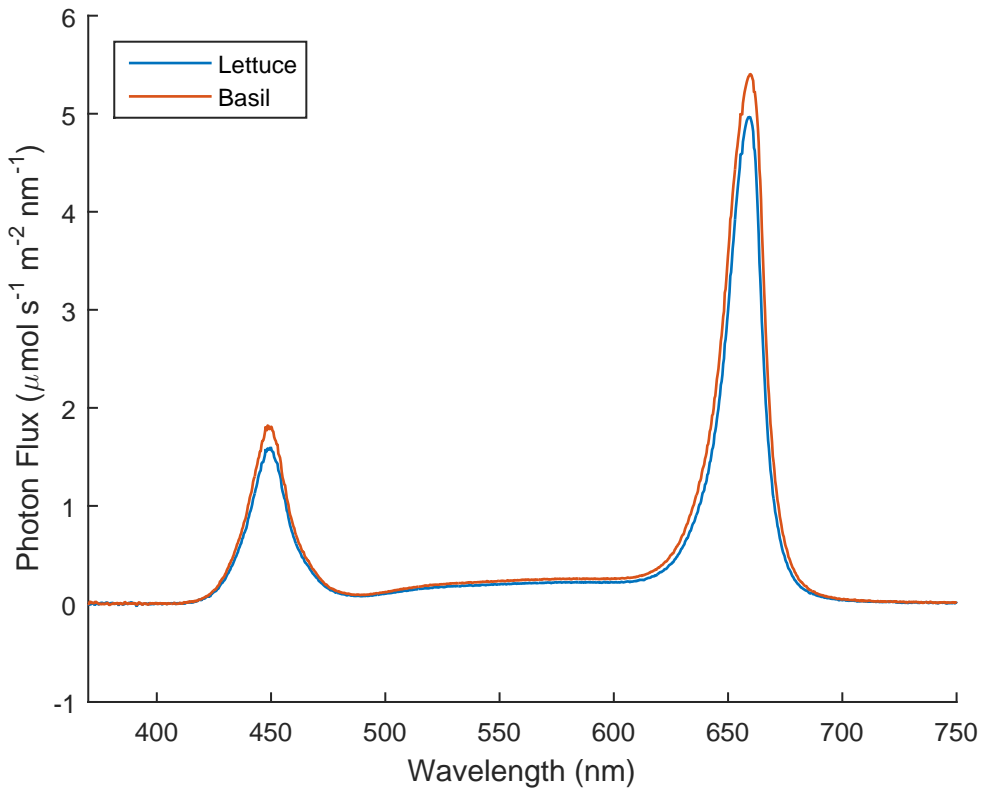


**Figure 4.6:** Spectra of the water stress experiment light regimes measured in the remote sensing unit.

#### 4.4.2 Remote sensing measurements

The fluorescence response and the incoming light were measured in the remote sensing unit. Two Maya2000 Pro spectrometers captured spectra with a sampling interval of 200 ms. The probe of the first spectrometer (M1) was placed in the middle of the unit facing up to measure the incoming light in PAR from the lamps. The height of the probe varied for different experiments to ensure that it was not shadowed by the plant canopy. The heights are presented in Table 4.6. The probe of the other spectrometer (M2) was mounted in between the lamps 84 cm above the metal grid, facing down onto the plant canopies to measure the chlorophyll *a* fluorescence.

#### 4.4.3 Reference measurements

In the light stress experiments and the water stress experiments reference measurements of plant physiology were taken using conventional methods. To this end, three Junior PAM fluorometers and one Pocket PEA fluorometer were used. The parameters measured are described in Table 2.1.

**Table 4.6:** Height of spectrometer M1 probe in different experiments, measured from the metal grid.

Experiment	Height
Light stress, lettuce	16.5 cm
Light stress, basil	16.5 cm
Complementary light stress, lettuce	16.5 cm
Complementary light stress, basil	18.5 cm
Water stress, draught, lettuce	16.5 cm
Water stress, moderate, lettuce	16.5 cm
Water stress, excessive, lettuce	16.5 cm
Water stress, draught, basil	21.5 cm
Water stress, moderate, basil	21.5 cm
Water stress, excessive, basil	21.5 cm

In the light stress experiments three plants, chosen at random, were monitored by the Junior PAMs for measurements of the parameters  $y(II)$  and  $NPQ$ . The latter requires measurements of the maximum fluorescence after dark adaptation of the sample. This dark adaptation was made prior to the experimental measurements, as the plants were kept in the reference measurement unit with the lamps turned off for 20 minutes. During the experiment samples were taken with an interval of 60 seconds. Furthermore, ten plants were randomly selected to be monitored by the Pocket PEA. Prior to the stress treatment leaf clips were used to dark adapt the samples for approximately 20 minutes and measurements of  $Fv/Fm$ ,  $PI$ ,  $Tfm$  and  $Area$  were taken. During the experiments the reference measurement unit was opened about 45 minutes into each level and Pocket PEA measurements were taken without dark adaptation. Without proper dark adaptation the instrument does not measure the parameters correctly, wherefore they are instead labelled  $Fv/Fm^*$ ,  $PI^*$ ,  $Tfm^*$  and  $Area^*$ . When put in relation to the correctly measured parameters taken before the experiment these parameters are assumed to carry information of the plant physiology development.

In the water stress experiments three plants were monitored by the Junior PAMs and thirteen were monitored by the Pocket PEA. Prior to the measurements taken in the remote sensing unit the samples were dark adapted for approximately 20 minutes. The Handy PEA were then used to measure parameters  $Fv/Fm$ ,  $PI$ ,  $Tfm$  and  $Area$  and the Junior PAMs measured  $Fv/Fm$ . Like in the light stress experiment these plants were chosen at random.

#### 4.4.4 Temperature measurements and fan control

The Heliospectra LX602 lamps used in the experimental units are equipped with a thermometer to measure the lamps circuit board temperature for temperature control. These temperatures were logged during the experimental measurements since the LEDs are assumed to have a temperature dependency. In the light stress experiments and the lettuce water stress experiment the set point of the lamps temperature control system was 25 °C. An unwanted behaviour caused by the bang-bang controller in the lamp was observed, where the light intensity of the LEDs was affected by the fan switching on and off. In the basil water stress experiment and both complementary light stress experiments this set point was therefore changed to 8 °C. The lower set point was infeasible resulting in fans running on full speed during the entire experiment, avoiding the on and off switching of the fans.

In the remote sensing unit a USBTemper was used to measure the air temperature in the unit.

### 4.5 Data treatment

The spectrometers used in the remote sensing unit collected five spectra per second each. To get the signals that were to be used in the system identification, the collected data had to be processed. All spectra were corrected with respect to dark-zero, electrical noise and temperature noise. To this end stored readings of dark-zero for each spectrometer and for different integration times, available at the company, were subtracted from the measurements.

Spectra of the measured incoming light were integrated over wavelengths 400 nm to 700 nm to get the incoming PAR as a function of time. Similarly, spectra measuring the fluorescence were integrated over wavelengths 730 nm to 750 nm to get the chlorophyll *a* fluorescence, with a peak at 740 nm, as a function of time.

Next, the signals were cut into pieces where each segment consisted of one step in the excitation signal from the lamps. The step responses were different for steps up and steps down, implying a non-linear system. Only the steps up were analysed in this work, and each step were treated and analysed individually. In all experiments, the first step at each light intensity level was discarded. This was due to the fact that the change in background light causes a response in chlorophyll fluorescence that interferes with the response caused by the excitation signal. Although this effect is not guaranteed to reach steady state before the second excitation step, it is assumed to be small enough to be treated as a linear trend. This linear trend was removed by subtracting a linear function fitted to the signals average value before the current and the closest following step. The last step at each level was discarded since there is no way to detrend that data using this procedure. After the detrending, all data segments were cut down to contain 100 data points (20 s) prior to the step and 300 data points (60 s) after the step.

The sampling interval 200 ms gave an approximate Nyquist frequency of 15.7 rad/s. In the previous work at the company [7] it was suggested that the most interesting

dynamics lies in the frequency range  $0.01 - 1$  rad/s, wherewith a low pass filter with cut-off frequency at 10% of the Nyquist frequency was found appropriate. Such a filter was realised by using a pseudo-Gaussian window function in the time domain

$$\hat{y}[k] = \frac{1}{2n+1} \sum_{i=-n}^n y[k+i]w[k+i]$$

with weights  $w[k]$  as presented in Figure 4.7. The filter is of non-causal finite response type. The non-causality of the filter is not considered a problem as it was only the sampling that was done in real time, with the data treatment and analysis being conducted off-line. The frequency response of the filter is presented in Figure 4.8, where the frequencies are normalised with respect to the Nyquist frequency  $\omega_N$ . The cut-off frequency of this filter is approximately  $0.1 \omega_N$ . It can be seen that the phase response of the filter is a linear function of frequency in the pass band of the filter. This *linear phase* property of the filter results in that all frequencies of the input signal are shifted in time by the same constant amount. In extension this means that there is no phase distortion due to the time delay of frequencies relative to one another [20].

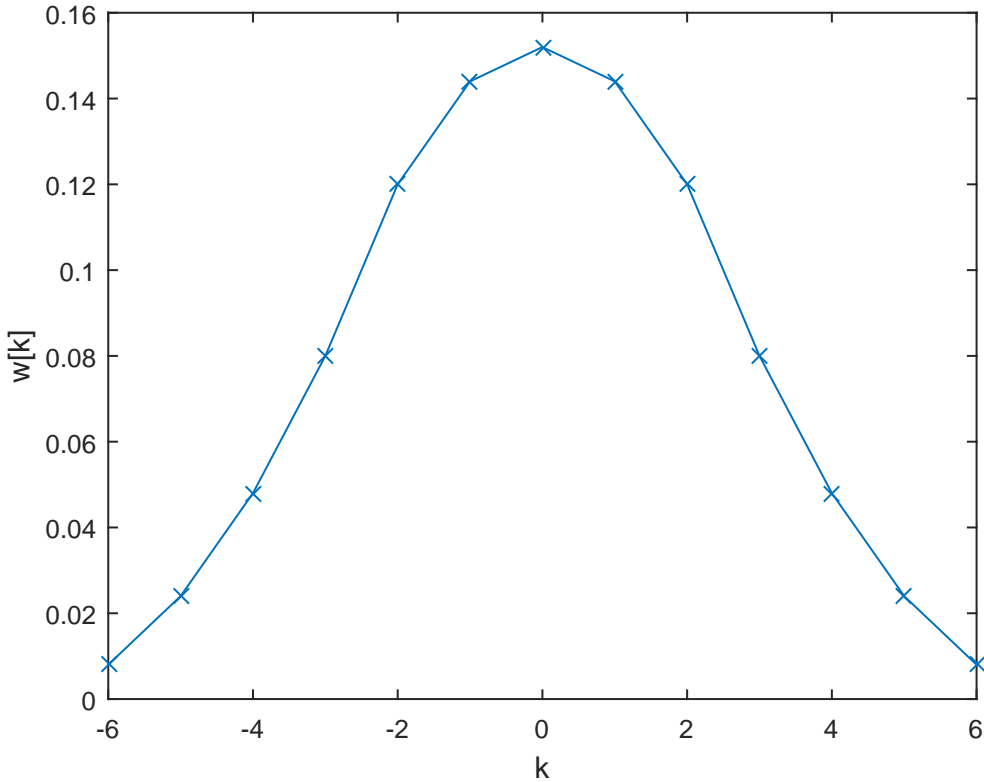


**Figure 4.7:** Pseudo-Gaussian weights of the discrete time low pass filter used in the data treatment procedure.

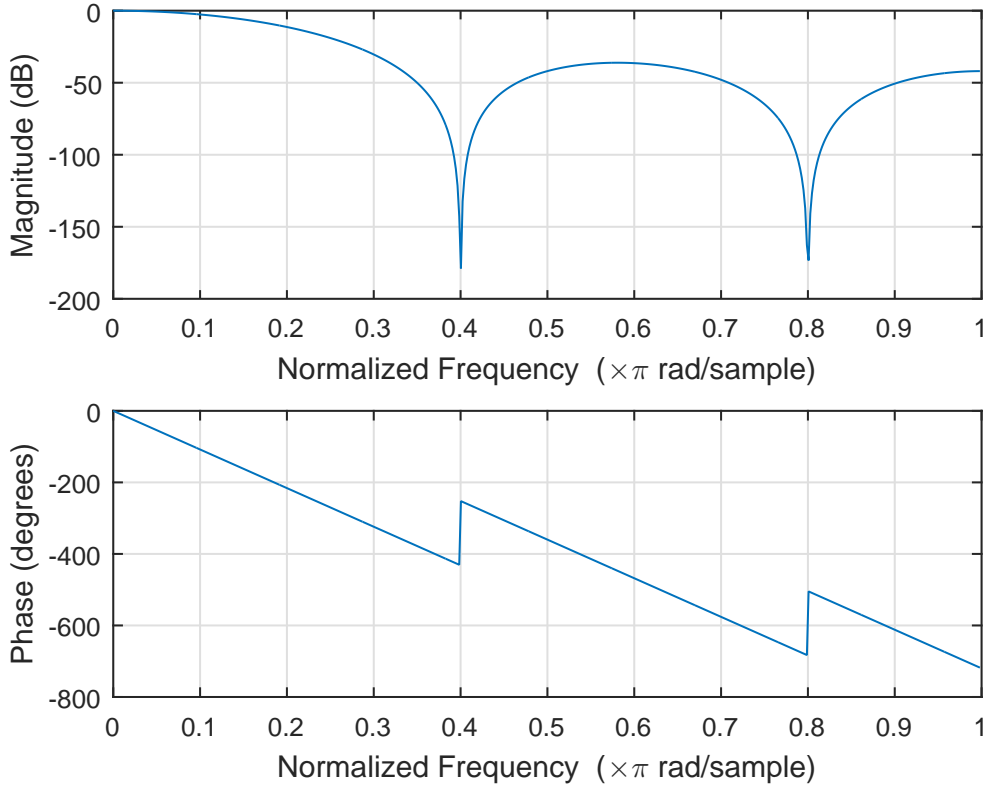


**Figure 4.8:** Frequency response of the discrete time low pass filter used in the data treatment procedure.

## 4.6 System identification

MATLAB's System Identification Toolbox was used to find suitable black-box models for each step response from the data treatment procedure. Each model is a linearised estimate of the real system for a certain operating point. In the previous work at the company [7], it was suggested that output error models with 3 – 4 poles and zeros were suitable to describe unstressed as well as stressed plants. It was also suggested that lower order models might be sufficient when the plants were stressed. This information was used as starting point in an iterative process to find model types and orders suitable for plants under different conditions.

For each step response measured different models were tried and evaluated. The performance of every model was reviewed based on how well it could simulate the measured behaviour of the system. The fit of the simulation to the measured data was calculated as

$$\text{fit}[\%] = 100 \left( 1 - \frac{\|y - \hat{y}\|}{\|y - \text{mean}(y)\|} \right),$$

where  $y$  is the measured output and  $\hat{y}$  is the simulated output. Visual inspection of the simulation was also important as the estimated models sometimes failed to capture important dynamics of the system behaviour. This could be a result of either a too low model order or a bad initial guess of output error model parameters. For output error models the parameter estimation procedure internally implemented in the System Identification Toolbox may get stuck in a local suboptimal estimate. This problem was dealt with by estimating every model twice. The first time no initial values were given. The parameters of the best performing model at each stress level were then used as initial value for the other systems at that level in the second estimation. If a better performing model was found in the second estimation, it replaced the original estimation. This procedure was automated and no manual inspection of the resulting estimates were needed. In some cases an alternative approach was used, where the initial values were set manually for each estimation. Three types of models were sought:

1. a model with as low order as possible that has a high fit percent that captures the most important system dynamics, and is robust in the sense that the automated estimation procedure works well for all systems investigated;
2. a model of lower order that is able to capture the most important dynamics of most of the systems investigated;
3. a model of lower order that is sufficient to describe the dynamics of the fluorescence response of stressed plants.

In the iterative process of finding a lower order model with sufficiently good performance, a higher order model was used for comparison. The Bode diagrams of the models were inspected and similar magnitude and phase plots for the relevant frequency band ( $0.01 - 1$  rad/s) indicated that the lower order model was sufficient. The poles and zeros of each system was also inspected as pole-zero cancellation may indicate an unnecessary high model order. Patterns of where the poles and zeros appeared were inspected. Systems measured at the same stress level was assumed to have relatively similar poles and zeros. Inconsistency of pole-zero placement between models that were expected to behave similarly was assumed to indicate modelling of less important system dynamics, motivating investigation of lower model orders.

# 5

## Results and discussion

**I**N THIS CHAPTER all results from the experiments as well as the data analysis are presented. In the first section signals from all the experiments, as measured in the remote sensing unit, are presented together with the temperatures that have been monitored. After that follows the results of the system identification process where suitable model orders are presented. Simulation results where these models have been used are presented for a selection of step responses. Then comes a section that presents the Bode plots of all systems modelled in all experiments. The Bode plots show clear trends that are compared to the reference stress measurements presented in the last section of this chapter.

### 5.1 Incoming light, fluorescence response and temperature measurements

This section presents the signals measured in the remote sensing unit for all experiments. This includes the incoming light in PAR (400 – 700 nm), the chlorophyll *a* fluorescence response (730 – 750 nm) and all temperatures.

The incoming light and the fluorescence response for the light stress experiments are shown in Figure 5.1. The quality of the incoming light signals and consequently the fluorescence responses during the fourth and fifth hour (light intensity levels 4 and 5) of the experiments are very poor as undesired, instant intensity changes appear. This behaviour coincide with major oscillations in lamp temperatures, as seen in Figure 5.2. The poor signal quality is thought to be a result of voltage drops over the lamps LED boards as the bang-bang controller in the temperature control system of the lamps switches on and off. The phenomenon also appears during the recovery phase, i.e. the eight hour of the experiment.

Figure 5.3 shows the incoming light and the fluorescence response for the complementary light stress experiments. The quality of the signals is good at all light intensity

levels. In these experiments the set point of the lamps temperature controller had been changed to suppress the temperature oscillations in the lamps, as mentioned in Section 4.4.4. The result is a more stable temperature development, depicted in Figure 5.4.

The measured signals and temperatures for the lettuce water stress experiment are presented in Figures 5.5 and 5.6. Three different measurements were taken for the three different stress groups (draught, moderate watering and excessive watering). In this experiment the set point of the lamps temperature controller had not yet been lowered and rather large temperature oscillations can be observed, resulting in poor (but handleable) signal quality. Figures 5.7 and 5.8 shows the corresponding measured signals and temperatures for the basil experiment, where the temperature oscillations are small and the signal quality is good.

In the light stress and the complementary light stress experiment the air temperatures in the remote unit, presented in Figures 5.2 and 5.4, are seen to increase as the intensity of the incoming light increases. This is an important observation to bare in mind as the stress in the plants might be partially caused by temperature. The air temperatures in the water stress experiments shown in Figures 5.6 and 5.8 are more stable and are assumed to have little impact on the plant stress.

It is clear from the plots presenting the incoming light (Figures 5.1, 5.3, 5.5 and 5.7) that the measured intensity levels do not agree with the intensity levels presented in Tables 4.3, 4.4 and 4.5. This is due to a problem with the spectrometer (M1) where the connection with the optical fibre is loose. The spectrometer and fibre were held fixed during the measurements to keep the connection stable, however no valid calibration file exists since a calibration would require an identical set up. The result is an incorrect scaling of the intensity. Furthermore, differences between the intensity of the measured incoming light are observed for light levels that are supposed to be equal between experiments. This is explained by varying plant geometry in the experimental units during the measurements as well as a varying height of the spectrometer probe (see Section 4.4.2). The conclusion is that signals of incoming light and fluorescence response should not be interpreted in terms of absolute values but rather in relative changes and relations to each other. The measured spikes in the beginning of the forth light level in the basil complementary light stress experiments, as seen in Figure 5.3, are explained by a poorly timed change of spectrometer integration time. These data points are discarded in the data treatment.

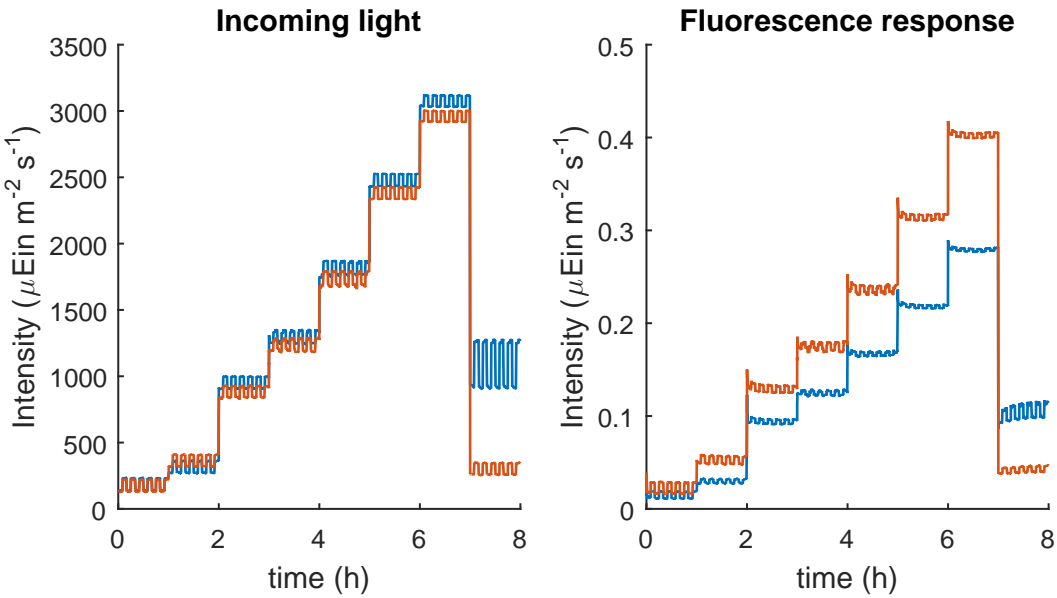


**Figure 5.1:** Measured incoming light in PAR (400 – 700 nm) and fluorescence response (730 – 750 nm) for lettuce (blue) and basil (red) in the light stress experiments.

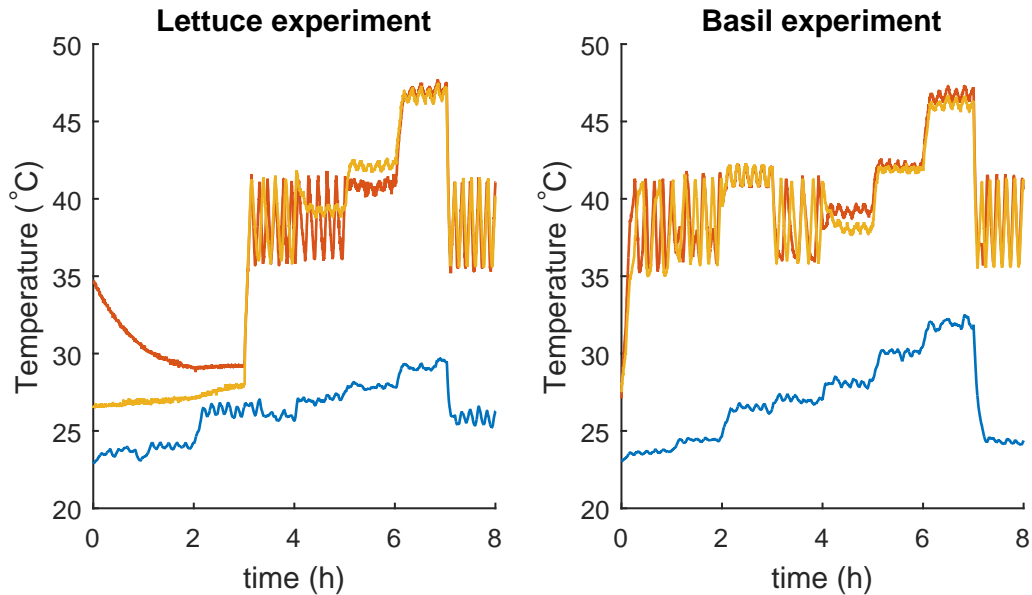


**Figure 5.2:** Air temperature (blue), remote unit lamp temperature (red) and reference unit lamp temperature (yellow) measured during the light stress experiments.

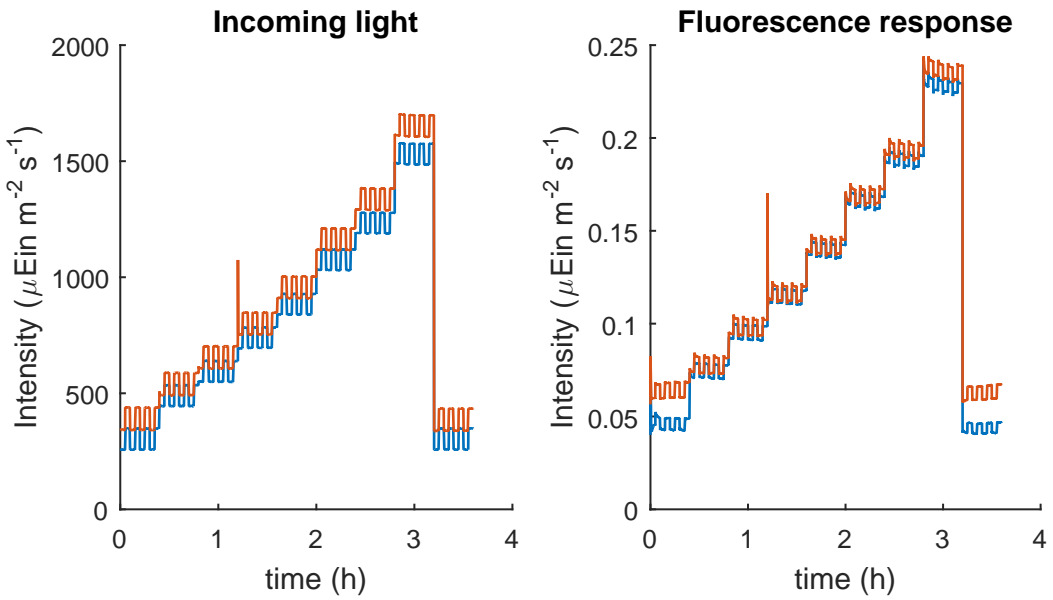


**Figure 5.3:** Measured incoming light in PAR (400 – 700 nm) and fluorescence response (730 – 750 nm) for lettuce (blue) and basil (red) in the complementary light stress experiments.

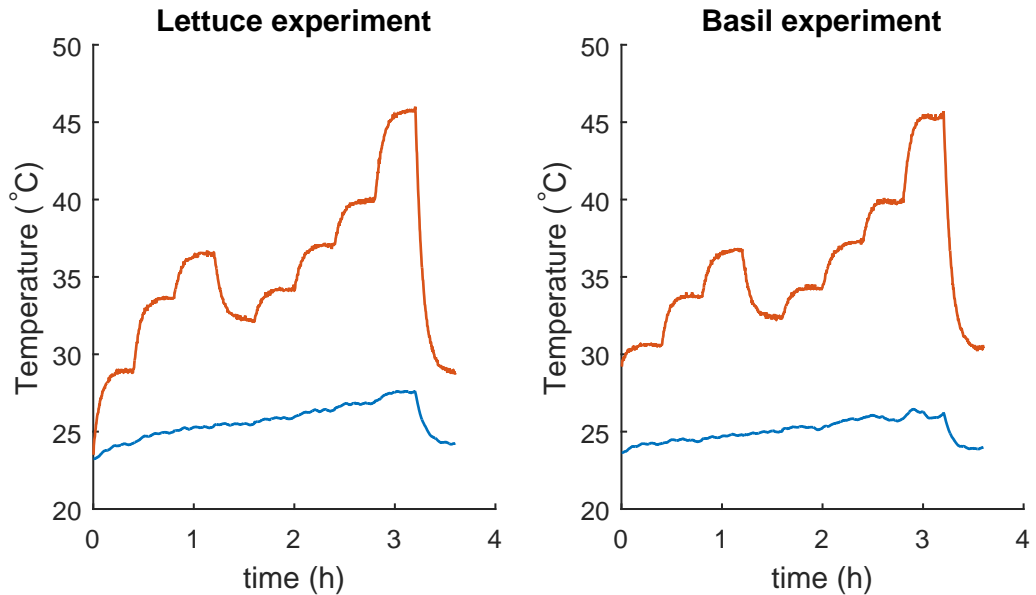


**Figure 5.4:** Air temperature (blue) and remote unit lamp temperature (red) measured during the complementary light stress experiments.

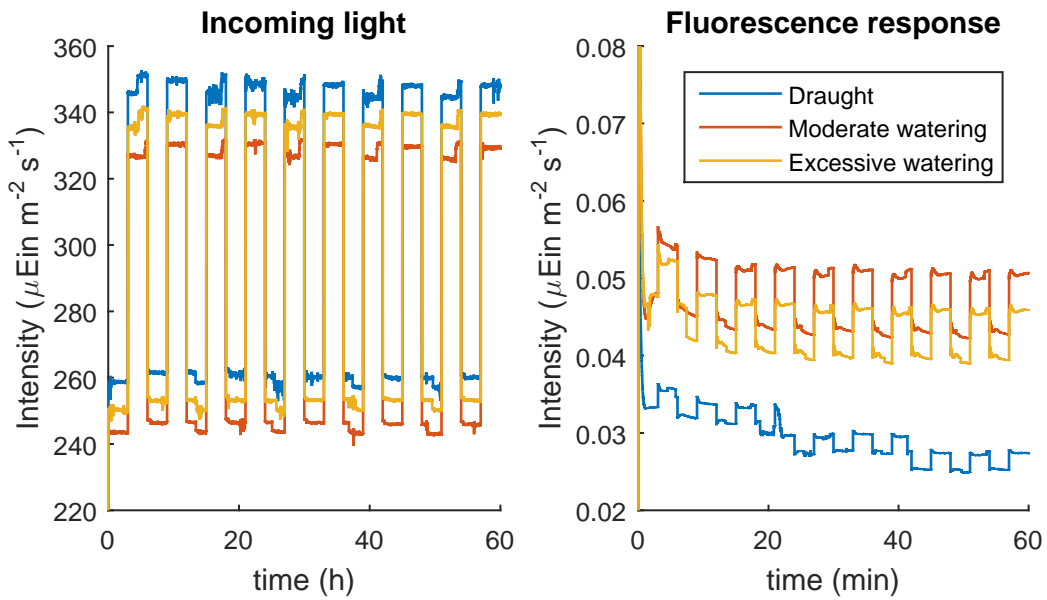


**Figure 5.5:** Measured incoming light in PAR (400 – 700 nm) and fluorescence response (730 – 750 nm) measured during the lettuce water stress experiments.

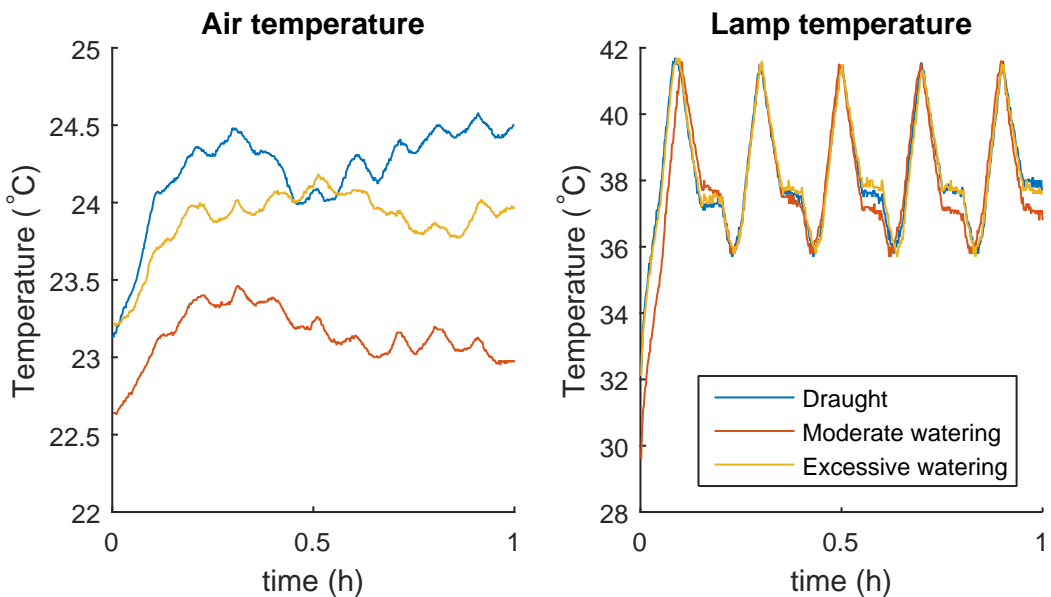


**Figure 5.6:** Air temperature and remote unit lamp temperature measured during the lettuce water stress experiments.

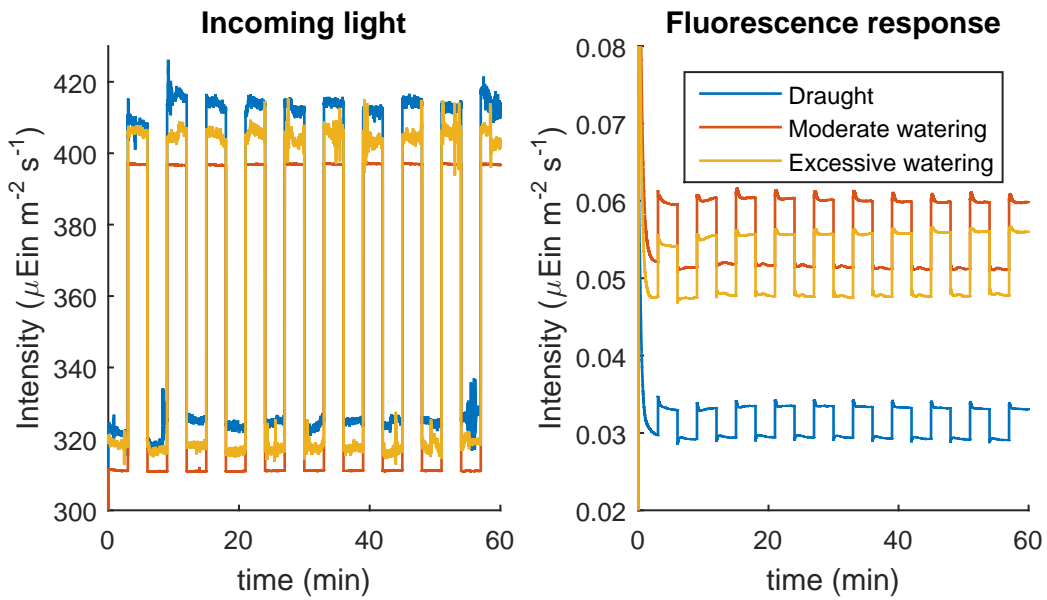


**Figure 5.7:** Measured incoming light in PAR (400 – 700 nm) and fluorescence response (730 – 750 nm) measured during the basil water stress experiments.

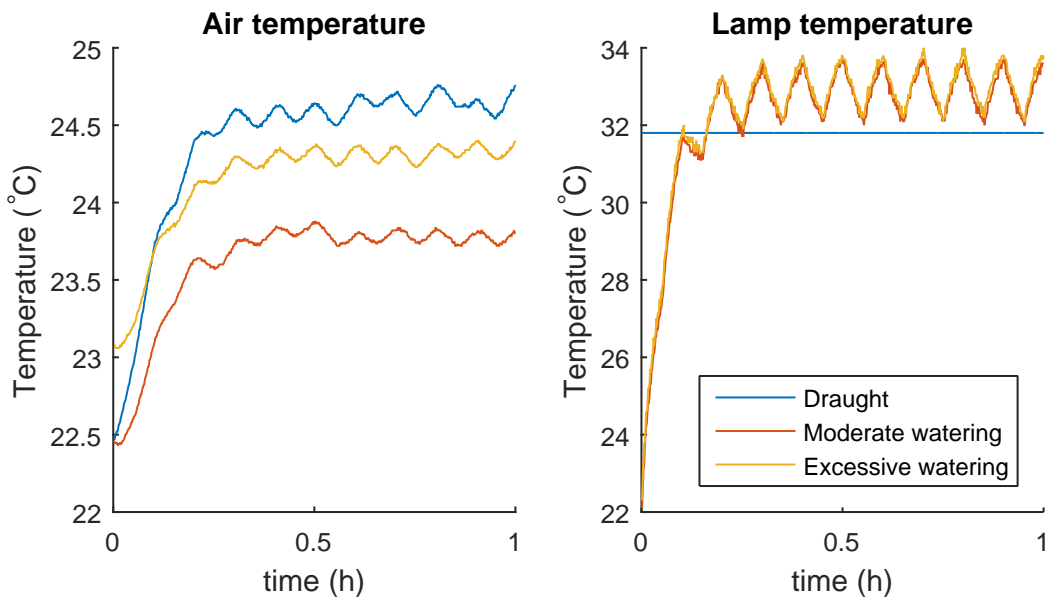


**Figure 5.8:** Air temperature and remote unit lamp temperature measured during the basil water stress experiments.

## 5.2 System identification

In the system identification process each set of steps of measured incoming light and fluorescence response was investigated and black-box models were fitted to the measured data. Upon visual inspection of the different step responses it was found that the overshoot occurred earlier and was more pronounced as the light intensity illuminating the plants increased. In Figure 5.9 three steps from the complementary light stress experiment on lettuce are chosen to visualise this trend. These steps exemplifies the results for both lettuce and basil in the light stress and the complementary light stress experiments.

Well watered plants under low light intensity is found to have a spike in fluorescence after about one second. This spike almost disappeared in the filtering process as it is more related to the fast part of the fluorescence transient, but it appears in the figures as a small bump at the end of the initial rise of the response. Under higher light intensities (or for plants subjected to draught) the spike coincide with the larger signal overshoot and is no longer identifiable. With faster sampling and/or less filtering it would be possible to investigate this spike in more detail, and it might carry information related to plant stress. It would however widen the frequency range in which the system is investigated towards higher frequencies where signal noise is a more significant problem. In this work such investigations were initially attempted by estimating systems without any data filtering. The results were, however, not satisfactory as the dynamics in the lower frequency range were compromised. For plants under very high light intensity, as investigated in the first light stress experiment (level 6 and 7), the overshoot was shown to be less pronounced and the dynamics appeared attenuated.

In the water stress experiments the overshoot appeared earlier and more pronounced for plants that had been subjected to draught. This is visualised in Figure 5.10 where three steps from the lettuce water stress experiment is presented. The results from the basil water stress experiment were very similar and are not visualised. It is seen that the difference between the moderately watered plants and the excessively watered plants is small. It seems likely that the excessively watered plants are not experiencing any water related stress. In fact they might be in better condition than the plants subjected to the moderate watering schedule. This hypothesis is supported by visual inspection of the plants shown in Figure 4.5, where one could argue that the excessively watered plants appears to be in better condition. This conclusion is simply based on the observation that these plants have grown more than the other groups.

Evaluation of different model orders, as described in Section 4.6, showed that an output error model with 3 poles, 3 zeros and a time delay of 1 sample was most suitable to achieve a high fit percent while keeping the model order relatively low. It was also found to be robust in the sense that estimations of such a models converged well in the automated system identification process for all steps investigated in this work. This model type is labelled oe431. A lower order model with 2 poles, 2 zeros and no time delay (oe320) was found sufficiently good to capture the most important dynamics of most systems, with the exception of the systems describing the recovery phase in the light stress experiment. It did perform slightly worse than the oe431 model in terms

of fit percent and it required visual inspection and manually set initial values in the system identification process. Systems with the faster dynamics (i.e. stressed plants) were found to be less complex and the model order could be reduced. In these cases a model with 1 pole, 1 zero and a time delay of 1 sample (oe211) gave sufficiently good estimations. Note that with a sampling interval of 200 ms the impact of a 1 sample time delay is small. The fast part of the transient response is known to be extremely fast (micro second scale) and with a 400 point data series being evaluated in the numerical estimation process a small offset during the rise time is negligible.

All steps measured in this work were estimated by models of type oe431, oe320 and oe211. The results of the estimations for the steps used to visualise trends in the complementary light stress experiment (Figure 5.9) are shown in Figure 5.11. It can be seen that the oe431 has the best fit percentage in all three simulations. The oe320 also has a good performance in these examples, but there were some problems when estimating oe320 models for the systems in the recovery phase. The oe211 model is not able to capture the most important dynamics of the system for the lower light intensity level but performs sufficiently well for the higher light intensity levels.

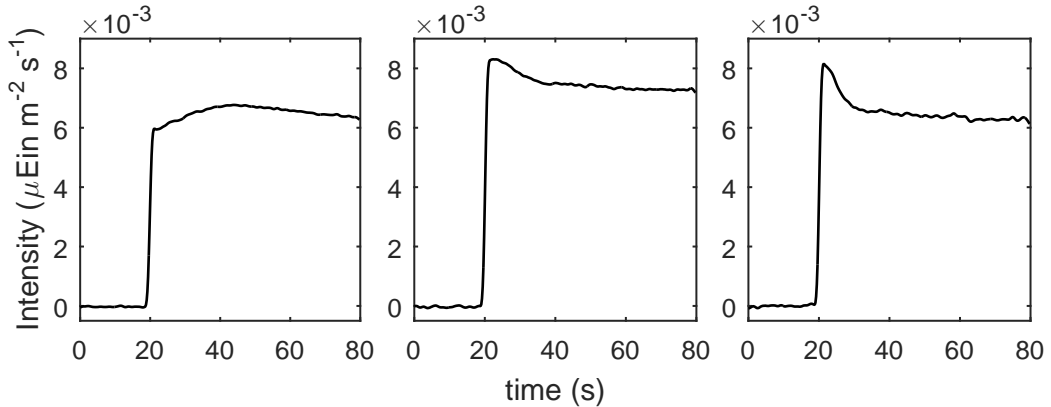


**Figure 5.9:** Filtered chlorophyll fluorescence responses for lettuce at three light intensity levels, measured in the complementary light stress experiment. One step from Level 11 (left), Level 3 (middle) and Level 6 (right) are shown. The levels are presented in detail in Table 4.4.

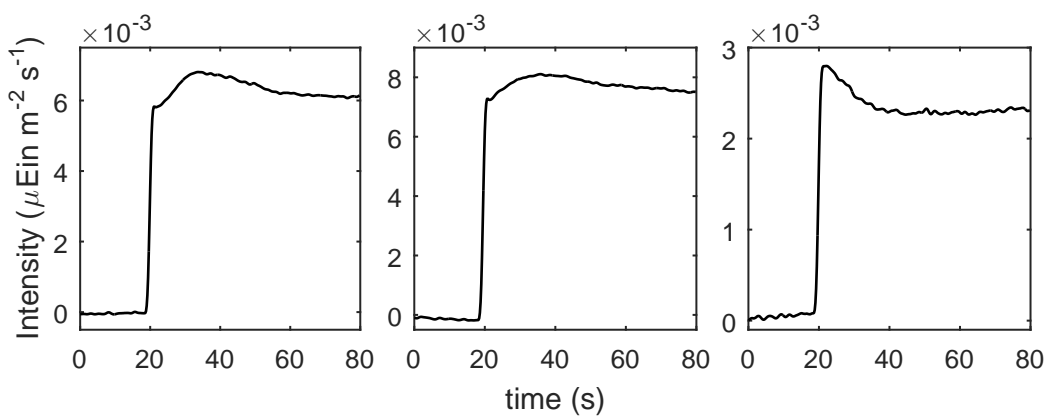


**Figure 5.10:** Filtered chlorophyll fluorescence responses for lettuce subjected to different watering schedules, measured in the water stress experiment. Excessive watering (left), Moderate watering (middle) and draught (right) are shown. During the measurements a light regime close to the one plants were grown under was used as background light.

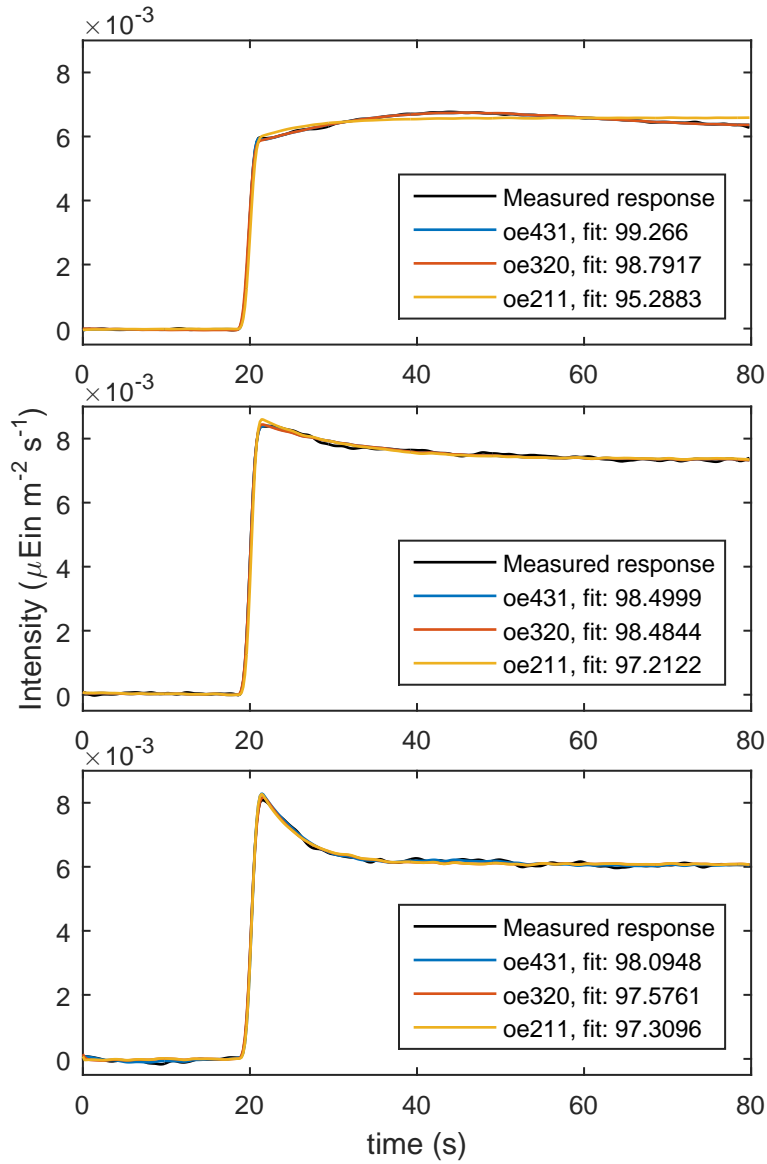


**Figure 5.11:** Simulation results of oe431, oe320 and oe211 models for three steps from the complementary light stress experiment, against the measured chlorophyll fluorescence response. The steps are from different light intensity levels: Level 11 (top), Level 3 (middle) and Level 6 (bottom). The measured data has been treated as described in Section 4.5.

### 5.3 Properties of the estimated systems

The systems estimated in the system identification part of this work were investigated in the frequency domain. For all systems, except those measured during the recovery phases of the light stress experiment, it was found that the Bode plots of systems estimated as oe431 and oe320 models looked very similar in the frequency range  $0.01 - 1$  rad/s. This lead to the conclusion that the oe320 model was sufficient to describe the system dynamics of those systems. During the recovery phase more complex dynamics were observed, as the spike during the fast rise of the fluorescence response was more pronounced. The larger oe431 model was needed to describe the dynamics during the recovery phase. In this section Bode plots of all models are presented. These diagrams reflects the behaviour of the system at different times. The magnitude plots are to be analysed with caution as the gain from incoming light to chlorophyll fluorescence is heavily dependent on the plant geometry in the experimental unit and the distance between the plant canopy and the spectrometer probe. The phase of the systems are assumed to be less sensitive to geometric factors, wherefore the phase plots of the models are considered suitable probes into the plants physiology.

Figure 5.12 and 5.13 shows the Bode plots from the light stress experiments. The levels refer to the different light intensity regimes listed in Table 4.3. All data (excluding reference measurements) from the fourth and fifth level were discarded due to the disturbances caused by the temperature oscillations in the lamps on these levels, which made the system estimation process unreliable. The Bode plots shows an interesting development as the light intensity increases. The phase is seen to increase for the midrange frequencies over the first three levels. For the two higher levels, where the light intensity is rather extreme, the phase have again decreased. When subjected to excessive lighting, plants are known to respond by realignment of chloroplast organelles to avoid light absorption [21]. This is one of many possible explanations of this behaviour. The higher light intensity levels also affects the signal to noise ratio of the measured chlorophyll fluorescence, explaining the more inconsistent system estimations at the higher levels.

In the basil experiment a drift in frequency is seen where the peaks of the plots appear at higher frequencies as the light intensity increases.

The behaviours of the systems during the recovery phase of the experiments are presented as Bode plots in Figures 5.14 and 5.15. It is seen that the recovery for basil can be tracked well by inspection of the Bode phase plot. The last system estimated in the recovery phase has a behaviour that is similar to that of the lower level systems, which is interpreted as a successful recovery. No such recovery can be observed in the lettuce experiment, which is explained by the high light intensity level of the recovery phase light regime.

Figures 5.16 and 5.17 shows the Bode plots from the complementary light stress experiments. In these experiments a different set of light intensity levels were used, which lie between the second and fifth level of the first light stress experiments as described in Table 4.4. Inspection of the lettuce phase plot shows a development that agrees very well with the first light stress experiment. The basil experiments also have similarities

between the two experiments, with a phase that increases for the midrange frequencies. However, the shift in frequency that was observed in the first light stress experiment is not reproduced in this experiment. Bode plots of the recovery phase in the complementary light stress experiments are shown in Figures 5.18 and 5.19. As in the first light stress experiment the recovery of the basil plants is shown to develop over time, with the last system resembling the ones shown for systems during the lower light levels. The lettuce however reacts much faster and shows a behaviour that does not match that of the systems during the lower light level to the same extent. It does however have more similarities with those systems than with the systems at higher light intensity levels. Comparison between the recovery phase in the complementary light stress is not relevant due to the difference in light regimes used in the two experiments.

Similar trends appear in the Bode plots for both of the light stress experiments, fortifying the relevance of the method investigated. The basil experiments also gives results similar to those presented in [7]. It is clear that the dynamics differ between lettuce and basil, implying that the slow phase dynamics differer between species.

Bode plots from the water stress experiments are shown in Figure 5.20 and 5.21. The plants subjected to different watering schedules is seen to behave differently in the low light regime used during the measurements. Comparison of the bode plots of the water stress experiments and light stress experiments indicate that the two different stress induction methods give rise to systems behaving very similar. The plants subjected to draught behaves similar in the low light intensity to how the plants under high light intensity levels do in the light stress experiments. This might suggest that it is the plants ability to utilise the incoming light that is measured, where a dried out plant does not have the same capacity as a fully watered plant. As previously discussed, inspection of the Bode plots indicates that the excessively watered plants are healthier than the moderately watered ones. This is motivated by the fact that the phase plots of the excessively watered plants resembles the phase plots from the lower light intensity levels in the light stress experiments.

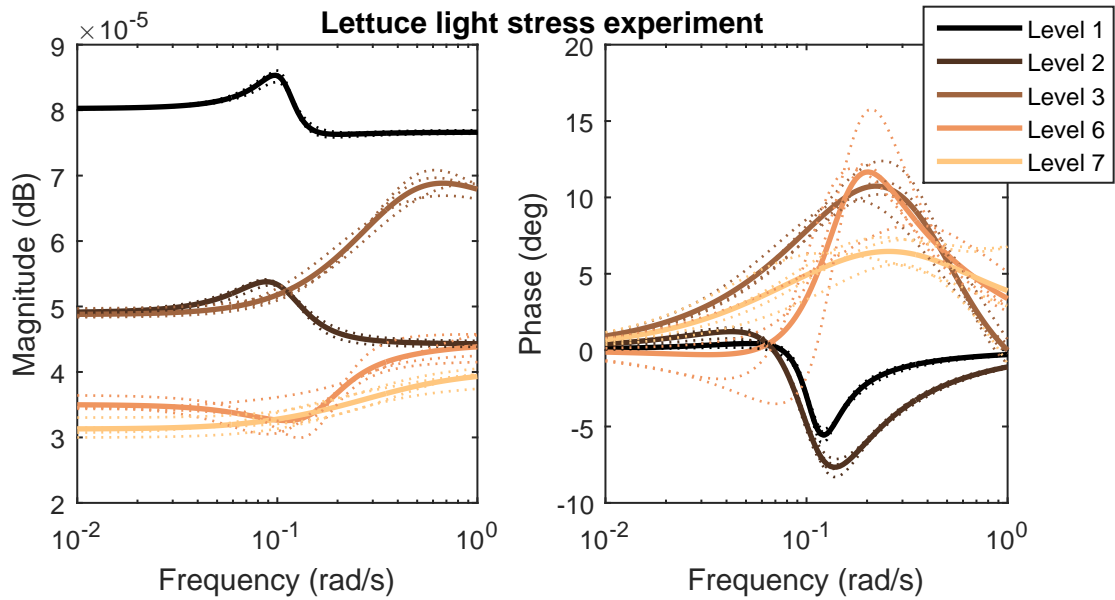


**Figure 5.12:** Bode plot of oe320 models estimated to each step response in the lettuce light stress experiment. Individual systems are presented as dashed lines and the average system at each level is presented as solid lines.

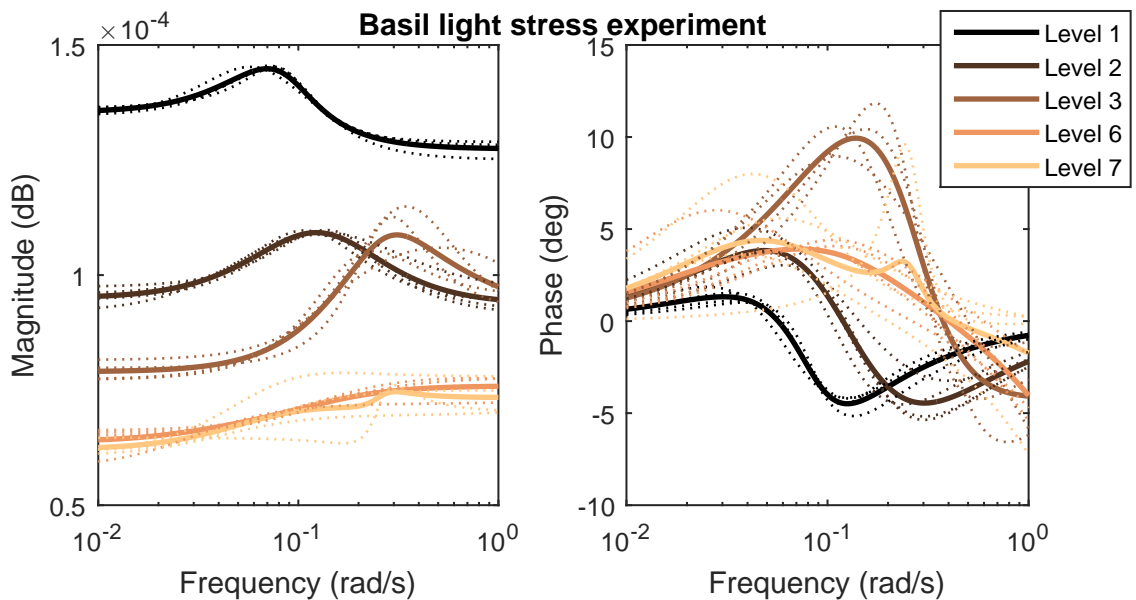


**Figure 5.13:** Bode plot of oe320 models estimated to each step response in the basil light stress experiment. Individual systems are presented as dashed lines and the average system at each level is presented as solid lines.

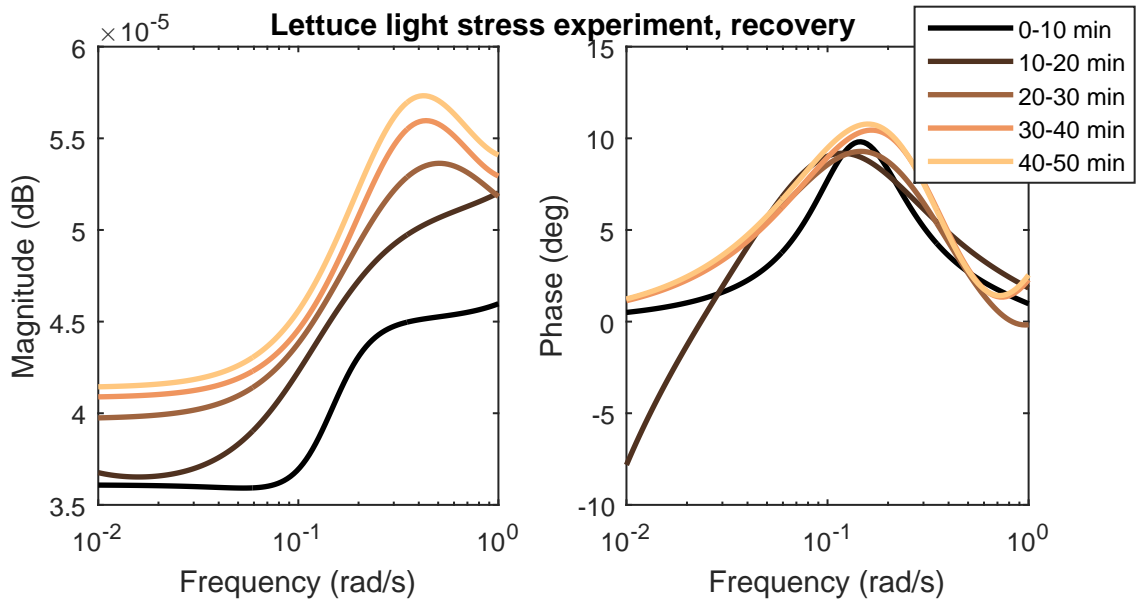


**Figure 5.14:** Bode plot of oe431 models estimated to each step response during the recovery phase in the lettuce light stress experiment.

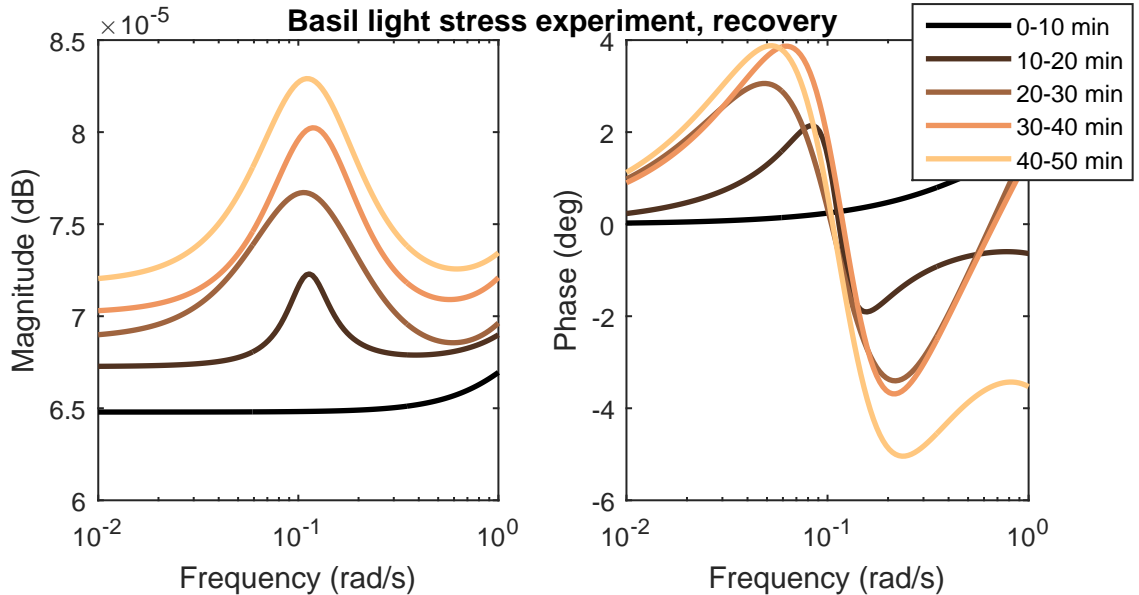


**Figure 5.15:** Bode plot of oe431 models estimated to each step response during the recovery phase in the basil light stress experiment.

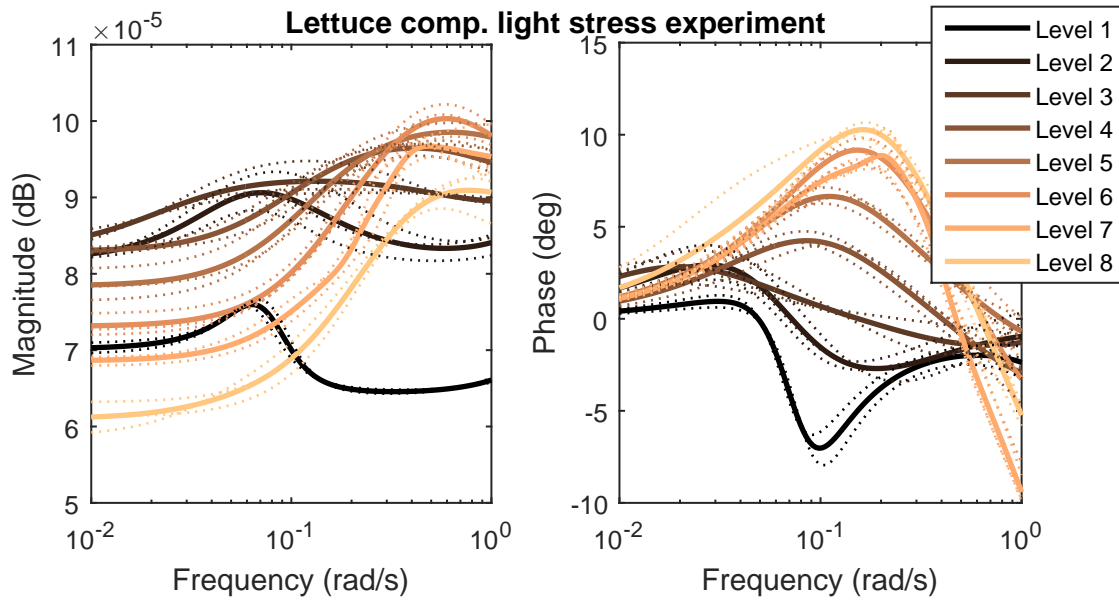


**Figure 5.16:** Bode plot of oe320 models estimated to each step response in the lettuce complementary light stress experiment. Individual systems are presented as dashed lines and the average system at each level is presented as solid lines.

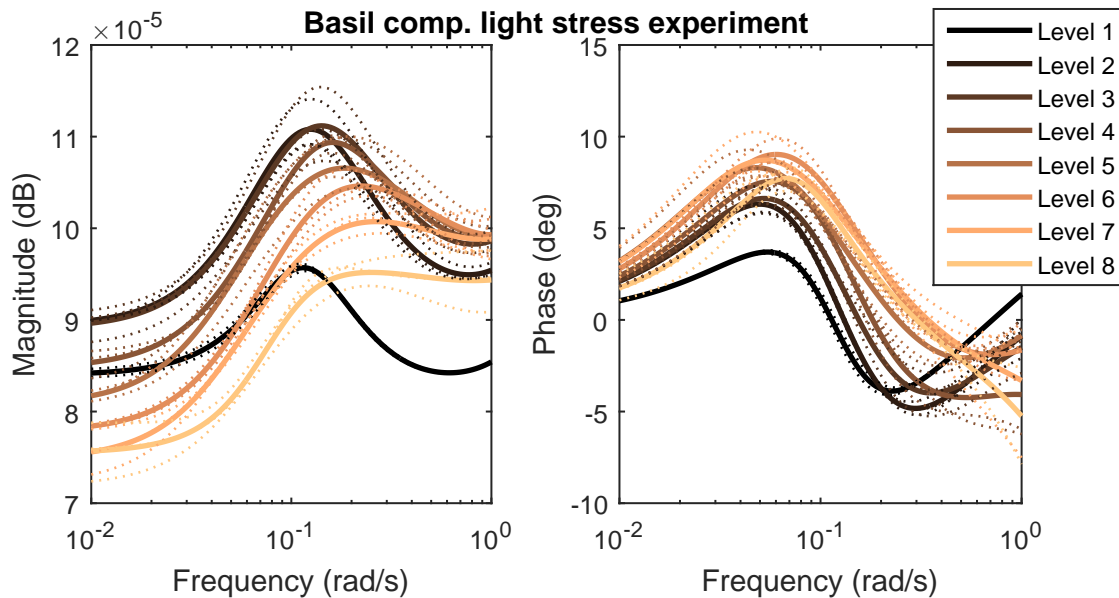


**Figure 5.17:** Bode plot of oe320 models estimated to each step response in the basil complementary light stress experiment. Individual systems are presented as dashed lines and the average system at each level is presented as solid lines.

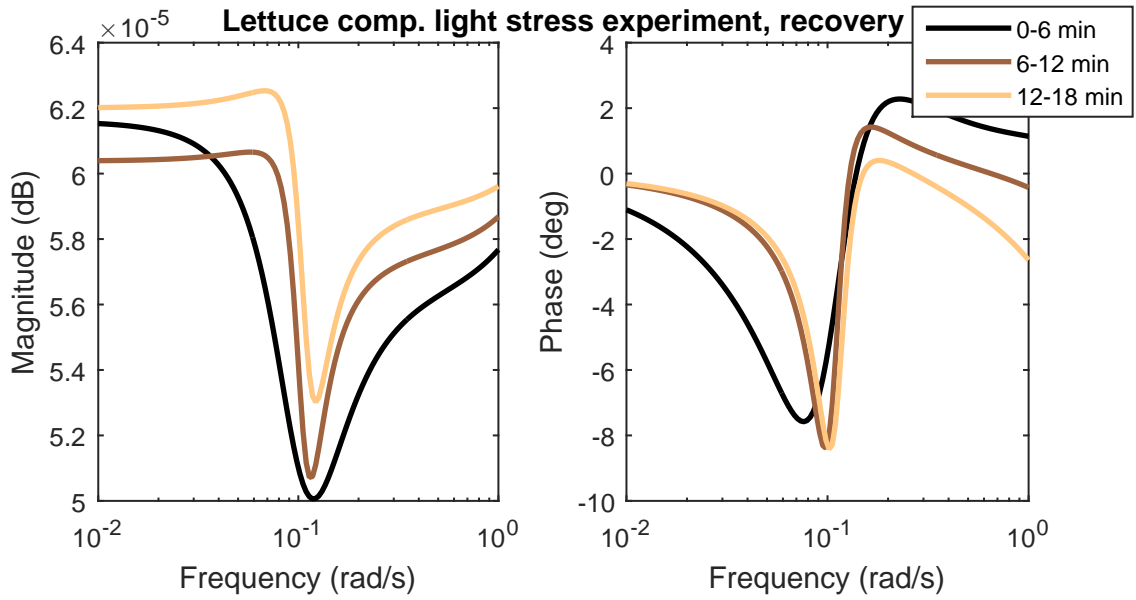


**Figure 5.18:** Bode plot of oe431 models estimated to each step response during the recovery phase in the complementary light stress experiment for lettuce.

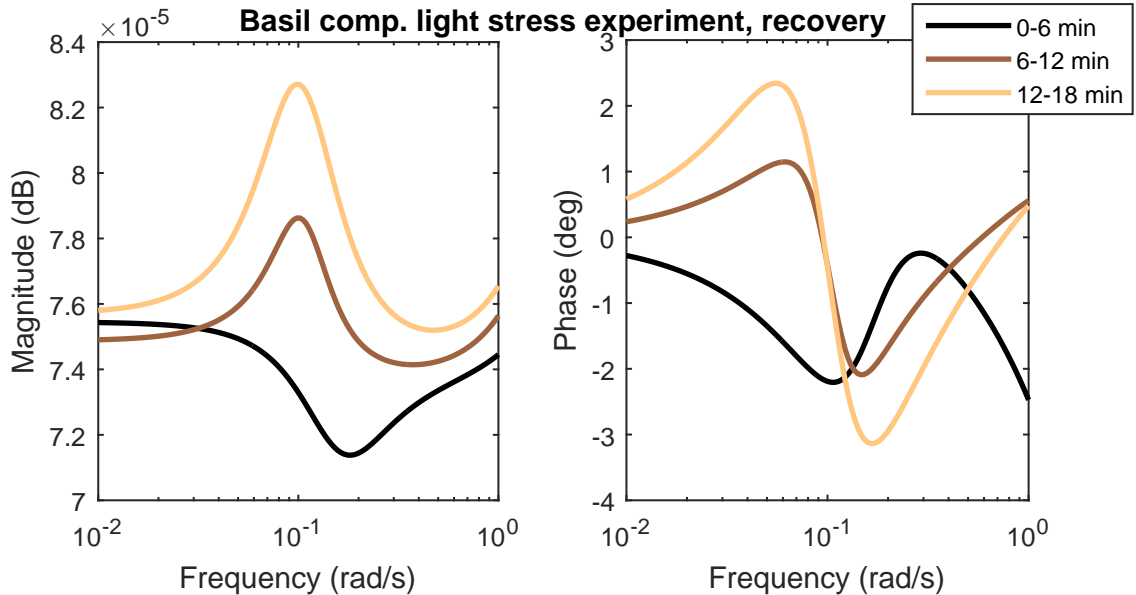


**Figure 5.19:** Bode plot of oe431 models estimated to each step response during the recovery phase in the complementary light stress experiment for basil.

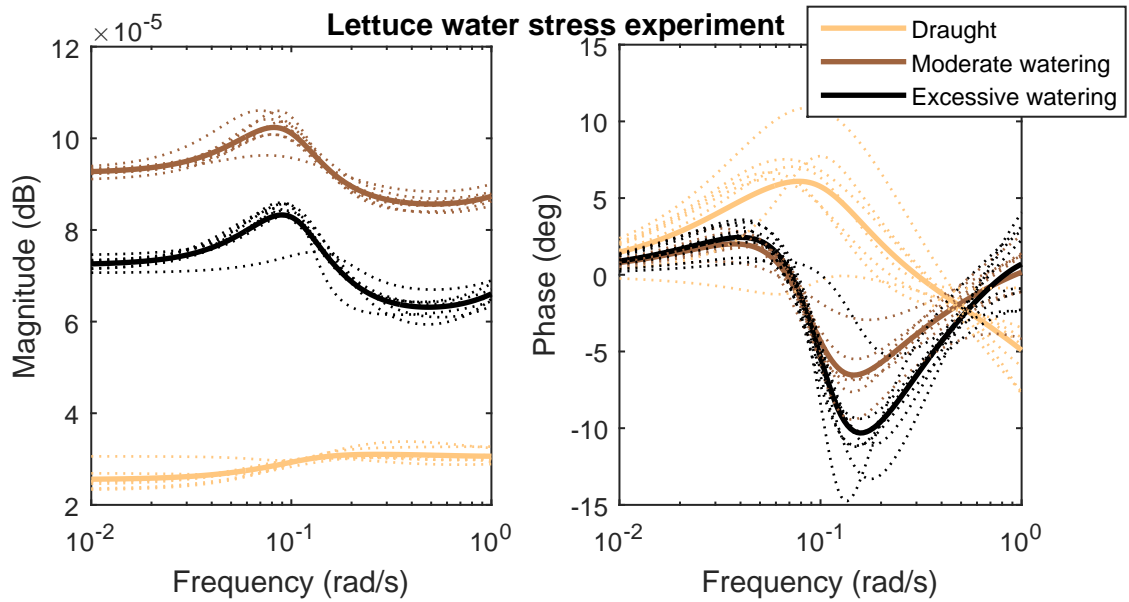


**Figure 5.20:** Bode plot of oe320 models estimated to each step response in the lettuce water stress experiment. Individual systems are presented as dashed lines and the average system at each level is presented as solid lines.

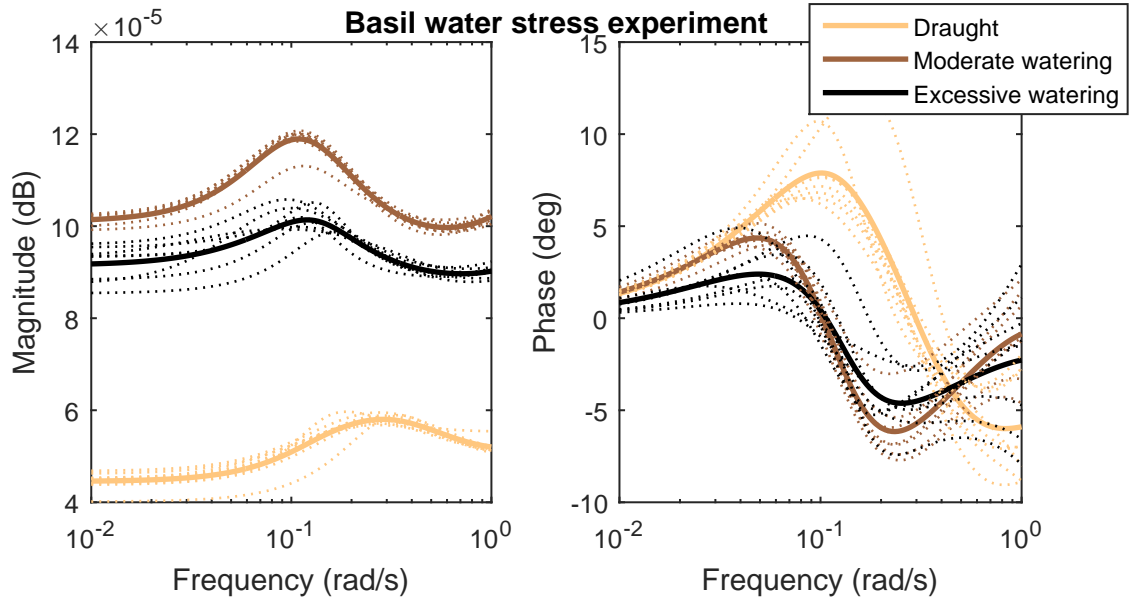


**Figure 5.21:** Bode plot of oe320 models estimated to each step response in the basil water stress experiment. Individual systems are presented as dashed lines and the average system at each level is presented as solid lines.

## 5.4 Reference measurements

In this section the parameters measured in the reference measurement unit during the experiments are presented. They were measured using a Handy PEA fluorometer and three Junior PAM fluorometers. These parameters reflect the physiology and stress level of the plants as described in Section 2.3.

### 5.4.1 Light stress experiments

The reference parameters  $F_V/F_M^*$ ,  $PI^*$  and  $y(II)$  measured in the light stress experiments on lettuce and basil are presented in Figures 5.22 and 5.23 respectively, together with the measurements of  $F_V/F_M$  and  $PI$  taken after dark adaptation prior to the experiment.

Measurements of the  $NPQ$  parameter was attempted using the Junior PAM fluorometers. The attempts failed since calculations of  $NPQ$  requires in-light measurements on the samples as well as measurements of the samples after dark adaptation. The dark adaptation was made prior to the experiment. However, during the several hour long in-light measuring period the geometry of the samples changed dramatically and comparison with measurements from the dark adapted samples was no longer relevant. Problems of plant stress measurements related to dark adaptation and leaf level measurements were expected and highlights the relevance of DFRA method investigated and developed in this thesis.

For both lettuce and basil the values of  $F_V/F_M$  as measured for the dark adapted plants lies close to or above 0.8 indicating that the plants are not stressed prior to the experiment. For the lower light intensity levels  $F_V/F_M^*$  has values relatively close to  $F_V/F_M$ , but for higher light intensities the value is decreasing. This is interpreted as an increased stress level in the plants. This is confirmed by inspection of the relationship between  $PI$  and the development of  $PI^*$  as well as the decreasing value of  $y(II)$ . The decreasing value of  $y(II)$  shows that during the higher light intensity levels a smaller fraction of the absorbed light is used for photochemical conversion. In an energy conservative greenhouse system this is clearly not desired. The recovery period at level 8 shows higher values of all parameters, implying a stress recovery. It can be seen that the basil plants are getting further in their recovery than the lettuce plants.

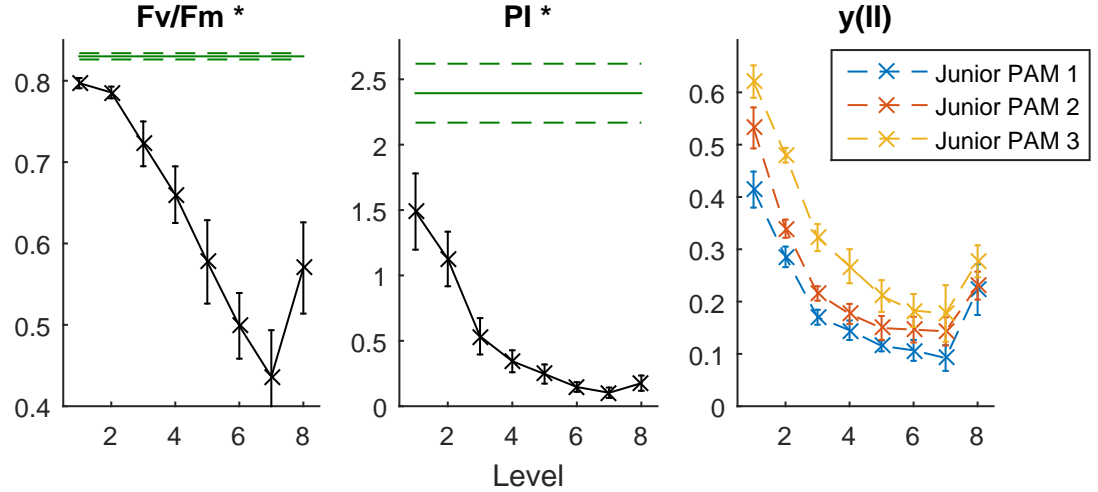


**Figure 5.22:** Measured reference parameters from the lettuce light stress experiment at the different light intensity levels. Averages (x) are presented with standard deviations. The left and middle plot shows Handy PEA measurements taken without dark adaptation. The green lines shows average measurements of corresponding parameters for dark adapted plants measured prior to the stress treatment, and the standard deviation. Data measured with the Junior PAMs are presented individually in the right plot as average values over the last fifteen minutes of every level.

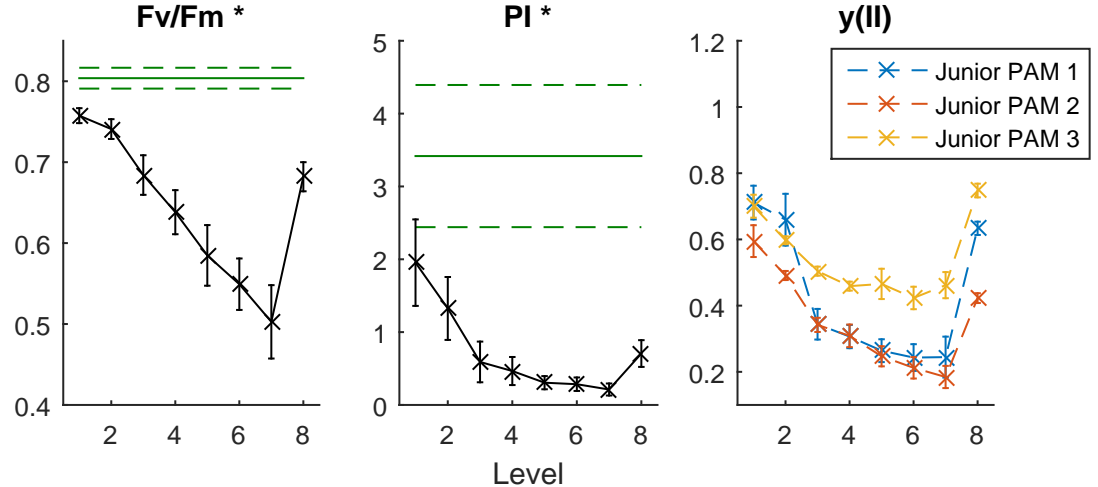


**Figure 5.23:** Measured reference parameters from the basil light stress experiment at the different light intensity levels. Averages (x) are presented with standard deviations. The left and middle plot shows Handy PEA measurements taken without dark adaptation. The green lines shows average measurements of corresponding parameters for dark adapted plants measured prior to the stress treatment, and the standard deviation. Data measured with the Junior PAMs are presented individually in the right plot as average values over the last fifteen minutes of every level.

### 5.4.2 Water stress experiments

The reference parameters  $F_V/F_M$  and  $PI$  measured in the water stress experiments on lettuce and basil are presented in Figures 5.24 and 5.25 respectively.

Both the Handy PEA and the Junior PAMs measured maximum quantum yield  $F_V/F_M$  well above 0.8 for all three stress groups, thus not indicating stress. A weak trend is observed where  $F_V/F_M$  is higher for plants subjected to draught which is counter intuitive as it indicates that those plants are healthier than the other groups. This trend is even more pronounced when inspecting  $PI$  which is significantly higher for the draught group.

In [11] it is concluded that mild water stress does not result in a dramatic loss of maximal photochemical activity ( $F_V/F_M$ ) of PSII, which is confirmed by the results of the water stress experiments.

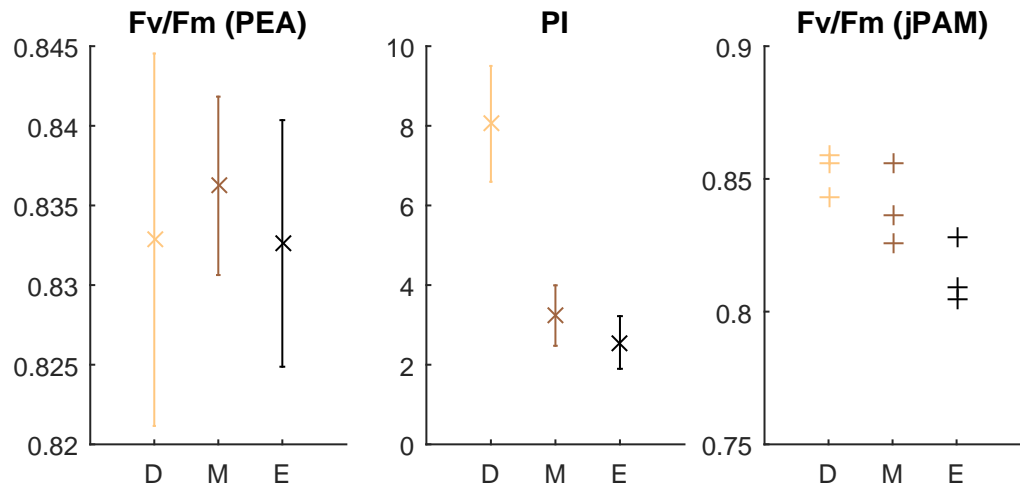


**Figure 5.24:** Measured reference parameters from the lettuce water stress experiment for plants subjected to draught (D), moderately watered plants (M) and excessively watered plant (E). Averages from Handy PEA measurements (x) are presented with their respective standard deviation. Data measured with Junior PAMs are presented individually (+).

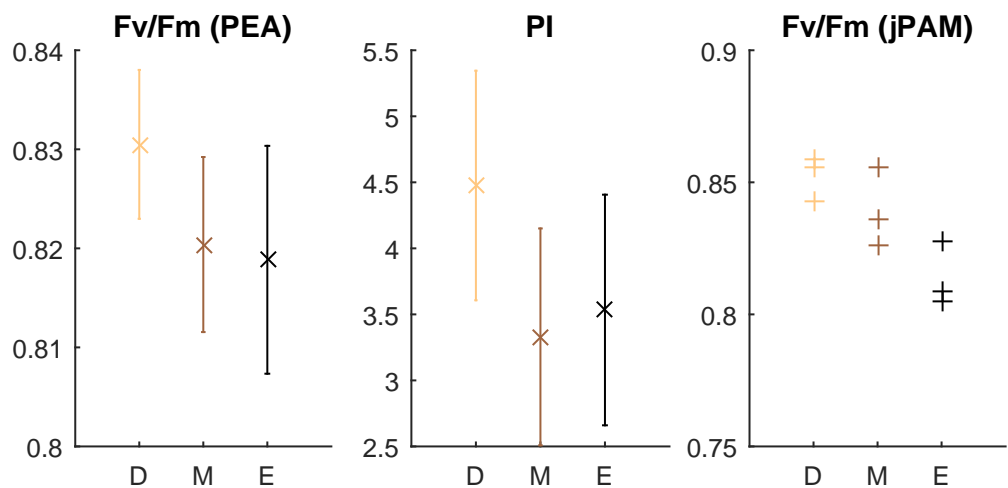


**Figure 5.25:** Measured reference parameters from the basil water stress experiment for plants subjected to draught (D), moderately watered plants (M) and excessively watered plant (E). Averages from Handy PEA measurements (x) are presented with their respective standard deviation. Data measured with Junior PAMs are presented individually (+).

## 5.5 Remote sensing versus reference measurements

To correlate the trends observed in the DFRA with the reference measurements, the Bode plots presented in Section 5.3 must be quantified. This is done by reading the phase value at 0.1 rad/s. The reference parameters are decreasing with stress whereas the phase is increasing, wherefore the reading of the phase is negated. The obtained quantity is denoted  $\Phi_{0.1}$  and is still measured in degrees. Figures 5.26 and 5.27 presents the reference measurements from the first light stress experiments plotted against PAR together with  $\Phi_{0.1}$  from the light stress and the complementary light stress experiment, also plotted against PAR. Comparing reference measurements from one experiment with  $\Phi_{0.1}$  measurements from another comes with the assumption that stress is induced in the plants similarly in both experiments. The  $F_V/F_M^*$  parameter is seen to decrease linearly with light intensity, whereas the  $PI^*$  and  $y(II)$  shows an exponential decay. This exponential decay is mimicked to some extent by the phase measurements from the DFRA method. For light intensities up to 600  $\mu\text{Ein}/\text{m}^2/\text{s}$  in PAR the  $\Phi_{0.1}$  correlates well with the reference measurements. This corresponds to light regimes about three times more intense than the regimes the samples are adjusted to. For higher intensities the  $\Phi_{0.1}$  parameter starts to increase, which does not agree with the reference measurements. Under such extreme conditions the DFRA method seems less appropriate. In an application where the remotely measured stress/photochemical efficiency is to be used as biological feedback, this result implies that the changes of light intensities must be sufficiently small so that the plant stress level is kept within the region where the DFRA method is reliable.

No quantification of the Bode plots from the water stress experiments are conducted, but as presented in Section 5.3 the effects of the different water treatments is clearly visible in the dynamics of the system. The trends agree well with how healthy the plants look upon visual inspection, as presented in the photographs in Figure 4.5. However, reference measurements of stress related parameters  $F_V/F_M$  and  $PI$  does not indicate any plant stress. The results suggest that the DFRA method, investigating the slow transient of a chlorophyll induction like curve, might be a suitable tool to measure water stress as well.

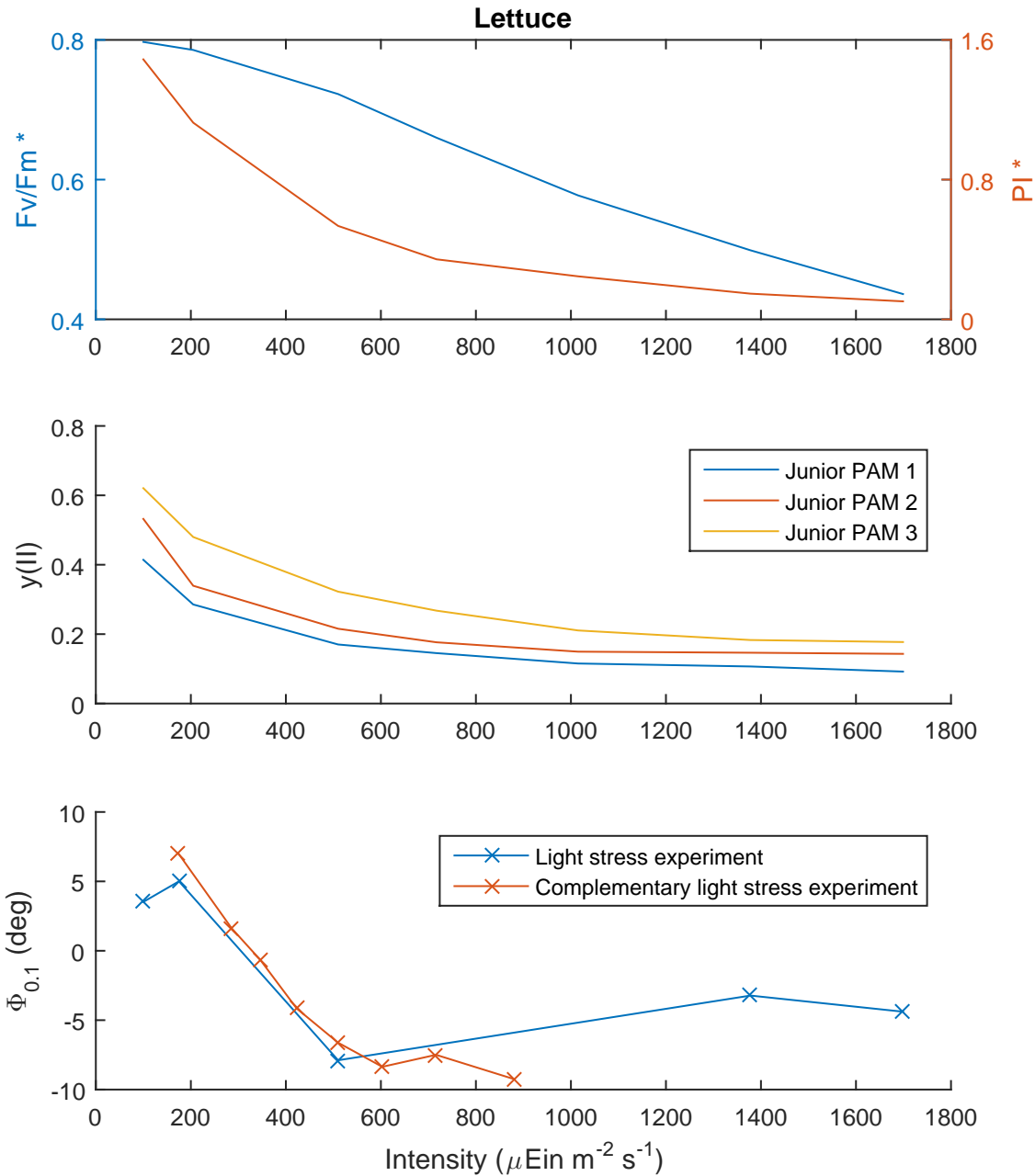


**Figure 5.26:** Top and middle plot shows reference measurements as functions of PAR from the lettuce light stress experiment. Bottom plot shows the negated phase measured at 0.1 rad/s as a function of PAR from the lettuce light stress and complementary light stress experiment.

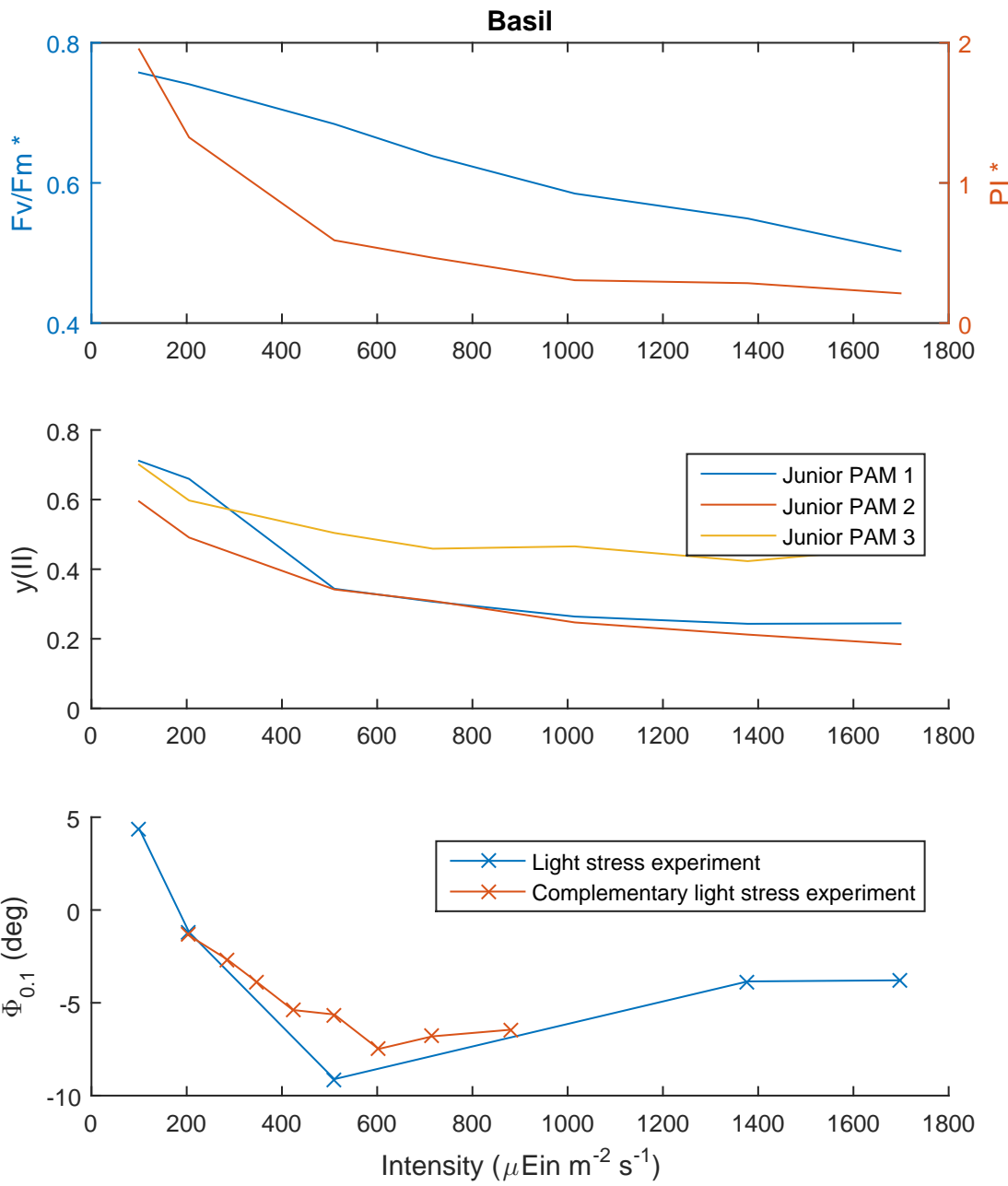


**Figure 5.27:** Top and middle plot shows reference measurements as functions of PAR from the basil light stress experiment. Bottom plot shows the negated phase measured at 0.1 rad/s as a function of PAR from the basil light stress and complementary light stress experiment.

# 6

## Conclusion

THE DYNAMIC FLUORESCENCE RESPONSE ANALYSIS method has been investigated and further developed in this work. It has been found that in order to model the dynamic fluorescence response in a robust way an output error model with three poles and three zeros is needed. Robust here means that the model type should be suitable for modelling the non-linear system for a wide range of operating points such as low stress environments, high stress environments and during stress recovery. If the recovery phase is excluded a smaller output error model with two poles and two zeros is sufficient to model the most important dynamics of the fluorescence response. It has been found that as the plants are getting more stressed the dynamics of the fluorescence response is getting less complex, and an even simpler output error model with only one pole and one zero can be used. A data treatment procedure has been presented that filters the measured data leaving information only in the frequency region important for DFRA.

The DFRA method has been deployed to investigate how plant stress and plant photosynthetic efficiency can be tracked for light stress and water stress in lettuce and basil. Inspection of the Bode plots of models estimated under different levels of stress shows trends that correlate well with reference parameters measured with conventional fluorometers. In particular the DFRA measurements could be used to track parameters related to photosynthetic efficiency by inspection of the Bode phase plot. For light stress, however, the method does only seem reliable under light intensity regimes that ranges from the intensity that the plants are adjusted to up to about three or four times more intense.

Similar trends appear in the Bode plots for light stress and water stress. The method does not seem appropriate to identify the type of stressor. However, by further extending the system with sensors monitoring environmental parameters such as soil moisture and temperatures, some stressors could be excluded.

With the ability to remotely track photosynthetic efficiency on canopy level in an

in-light environment, the DFRA method could be applied for biological feedback when controlling the lighting in greenhouses. Also, by using external sensors monitoring environmental parameters such as soil moisture, air temperature etc certain stressors could be . Further work should be conducted to find suitable set points for the phase, that translates to an optimal photosynthetic efficiency. To this end, more stressors and/or more plant species should be investigated.

All investigations in this work has been conducted in a closed environment, with no disturbing light source. In an open greenhouse environment a major part of the illumination will come from the sun. To be able to apply the DFRA method under such conditions the method needs to be extended with an algorithm to compensate for such disturbances.

# Bibliography

- [1] L. Ahlman, D. Båkestad, and T. Wik, “Using chlorophyll *a* fluorescence gains to optimize led light spectrum for short term photosynthesis,” *Computers and Electronics in Agriculture*, Submitted.
- [2] Govindjee, “Chlorophyll *a* fluorescence: A bit of basics and history,” in *Chlorophyll *a* Fluorescence - A Signature of Photosynthesis* (G. C. Papageorgiou and Govindjee, eds.), vol. 19 of *Advances in Photosynthesis and Respiration*, Springer Netherlands, 2004.
- [3] Hansatech Instruments Ltd, *Operations Manual - Setup, Installation and Maintenance - Handy PEA, Pocket PEA and PEA Plus Software*, 2006.
- [4] Heinz Walz GmbH, *Junior-PAM - Chlorophyll fluorometer Operator's Guide*, 2007.
- [5] I. Moya and Z. G. Cerovic, “Remote sensing of chlorophyll fluorescence: Instrumentation and analysis,” in *Chlorophyll *a* Fluorescence - A Signature of Photosynthesis* (G. C. Papageorgiou and Govindjee, eds.), vol. 19 of *Advances in Photosynthesis and Respiration*, Springer Netherlands, 2004.
- [6] Z. Malenovsky, K. B. Mishra, F. Zemek, U. Rascher, and L. Nedbal, “Scientific and technical challenges in remote sensing of plant canopy reflectance and fluorescence,” *Journal of Experimental Botany*, vol. 60, no. 11, pp. 2987–3004, 2009.
- [7] A.-M. Carstensen, T. Wik, and T. Pocock, “Remote detection of light induced stress in basil through the dynamic behaviour of light induced fluorescence,” *Journal of remote sensing of environment*, Submitted.
- [8] R. Kaňa, O. Komárek, E. Kotabová, G. C. Papageorgiou, Govindjee, and O. Prášil, “The slow S to M fluorescence rise is missing in the RpaC mutant of *synechocystis* sp. (PCC 6803),” in *Photosynthesis Research for Food, Fuel and Future - 15th International Conference on Photosynthesis* (L. C. Z. Kuang, Tingyun and Lixin, eds.), Advanced Topics in Science and Technology in China, Springer-Verlag Berlin Heidelberg, 2013.

- [9] C. W. Mullineaux and D. Emlyn-Jones, "Scientific and technical challenges in remote sensing of plant canopy reflectance and fluorescence," *Journal of Experimental Botany*, vol. 56, no. 411, pp. 389–393, 2005.
- [10] H.-W. Trissl, Y. Gao, and K. Wulf, "Theoretical fluorescence induction curves derived from coupled differential equations describing the primary photochemistry of photosystem II by an exciton-radical pair equilibrium," *Biophys Journal*, vol. 64, no. 4, p. 974–988, 1993.
- [11] N. G. Bukhov and R. Carpentier, "Effects of water stress on the photosynthetic efficiency of plants," in *Chlorophyll a Fluorescence - A Signature of Photosynthesis* (G. C. Papageorgiou and Govindjee, eds.), vol. 19 of *Advances in Photosynthesis and Respiration*, Springer Netherlands, 2004.
- [12] A. Stirbet, G. Y. Riznichenko, A. B. Rubin, and Govindjee, "Modeling chlorophyll a fluorescence transient: Relation to photosynthesis," *Biochemistry (Moscow)*, vol. 79, no. 4, pp. 379–412, 2014.
- [13] R. J. Strasser, A. Srivastava, and M. Tsimilli-Michael, "Analysis of the fluorescence transient," in *Probing Photosynthesis: Mechanism, Regulation and Adaptation* (M. Yunus, U. Pathre, and P. Mohanty, eds.), London, UK: Taylor and Francis, 2000.
- [14] M. Ashraf and P. J. C. Harris, "Photosynthesis under stressful environments: An overview," *Photosynthetica*, vol. 51, no. 2, pp. 163–190, 2013.
- [15] T. Shepherd and D. W. Griffiths, "The effects of stress on plant cuticular waxes," *New Phytologist*, vol. 171, no. 3, pp. 469–499, 2006.
- [16] H. Lepeduš, I. Brkić, V. Cesar, V. Jurković, J. Antunović, A. Jambrović, J. Brkić, and D. Šimić, "Chlorophyll fluorescence analysis of photosynthetic performance in seven maize inbred lines under water-limited conditions," *Periodicum Biologorum*, vol. 114, no. 1, pp. 73–76, 2012.
- [17] D. J. DeFatta, J. G. Lucas, and W. S. Hodgkiss, *Digital signal processing: A system design approach*. John Wiley and Sons, 1988.
- [18] L. Ljung and T. Glad, *Modelling of Dynamic Systems*. PTR Prentice Hall, 1994.
- [19] D. Bänkestad, "Optimisation of led lighting in greenhouses by remote sensing of plant reflectance and fluorescence," Master's thesis, Chalmers university of technology, 2013.
- [20] J. O. Smith, *Introduction to Digital Filters: with Audio Applications*. W3K Publishing, 2007.
- [21] Z. Li, S. Wakao, B. B. Fischer, and K. K. Niyogi, "Sensing and responding to excess light," *Annual Review of Plant Biology*, vol. 60, pp. 239–260, 2009.